Koninklijke Sterrenwacht van België
Observatoire royal de Belgique
Royal Observatory of Belgium

Jaarverslag 2011
Rapport Annuel 2011
Annual Report 2011

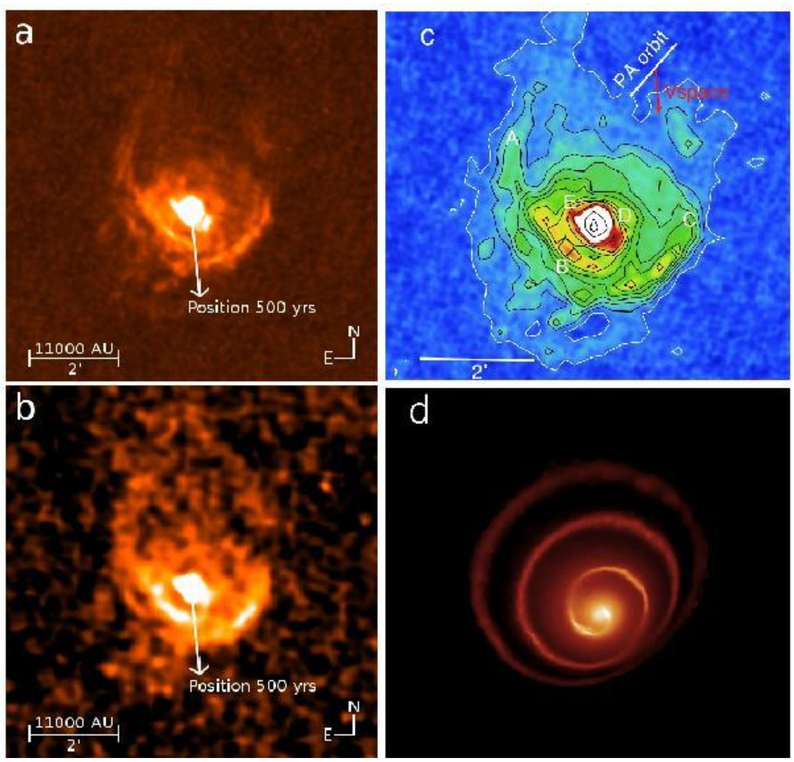

Mensen voor Aarde en Ruimte, Aarde en Ruimte voor Mensen
Des hommes et des femmes pour la Terre et l'Espace, La Terre et l'Espace pour l'Homme

Cover illustration : Herschel's view into Mira's head (Mayer, … Groenewegen, et al., 2011, A&A)

De activiteiten beschreven in dit verslag werden ondersteund door
Les activités décrites dans ce rapport ont été soutenues par
The activities described in this report were supported by

De POD Wetenschapsbeleid
Le SPP Politique Scientifique

De Nationale Loterij
La Loterie Nationale

Het Europees Ruimtevaartagentschap
L'Agence Spatiale Européenne

De Europese Gemeenschap
La Communauté Européenne

Het Fonds voor Wetenschappelijk Onderzoek – Vlaanderen

Le Fonds de la Recherche Scientifique

Table of Contents

Preface ... ***5***
Reference Systems and Planetology ... ***6***
Using Global Navigation Satellite Systems (GNSS) for science and services ... 7
Earth Rotation ... 10
Geodesy and Geophysics of Terrestrial Planets ... 11
Time – Time Transfer ... 16
Gravimetry & Seismology ... ***18***
Composite Seismogenic Source Model in the Valley Rift System ... 19
Crustal Structure at the Princess Elisabeth Base in Antarctica ... 20
The volcanic hydrothermal system of Kawah Ijen in Indonesia ... 21
The Seismic Alert System ... 22
Absolute Gravity measurements to measure deformation of the Lithosphere in Northwest Europe ... 23
Astronomy & Astrophysics ... ***24***
Stellar Astrophysics: Asteroseismology ... 25
Gaia: The Billion Star Surveyor ... 27
Late evolution phases and mass loss ... 29
Solar Physics and Space Weather ... ***32***
3D Stereo Work & Linking in-situ with Remote Sensing ... 33
A small-sunspot deficit in solar cycle 23 ... 35
Detection and Tracking of Active Regions and Coronal Holes ... 37
Radio Observations in Humain ... 38
The Planetarium ... ***42***
Information services ... ***46***
Annex 1: Refereed Publications 2011 ... ***48***
Annex 2: Human Resources 2011 ... ***58***

Preface

This report describes the highlights of scientific activities and public services at the Royal Observatory of Belgium in 2011.

A list of publications and the list of personnel is included at the end.

Due to lack of means and personnel the report is only in English. A description of the most striking highlights is available in Dutch and French.

If you need more or other information on the Royal Observatory of Belgium and/or its activities please contact rob_info@oma.be or visit our website http://www.astro.oma.be.

Kind regards
Ronald Van der Linden
Director General

Reference Systems and Planetology

Using Global Navigation Satellite Systems (GNSS) for science and services

The GNSS team uses GPS data and more generally Global Navigation Satellite System (GNSS) data in order to determine precise positions (at the mm level) and deformation/velocities (at the sub-mm/year level). This allows them to characterize regional and global ground deformations and to integrate Belgium in international terrestrial coordinate reference systems. This is performed through the integration of several continuously observing GNSS reference stations and associated services in international GNSS observation networks. The 'GNSS' ROB team contributes actively to the European and global developments of GNSS observation networks, their products and applications since more than ten years. This has resulted in a number of responsibilities within the International GNSS Service (IGS) and the EUREF (European Reference Frame) Permanent GNSS Network (EPN). The EPN is a network of almost 250 permanently observing GNSS stations distributed all over Europe which is managed by the ROB GNSS team (http://www.epncb.oma.be; it received about 2.5 million hits in 2011). The EPN is the foundation of the European Terrestrial Reference System (ETRS89) recommended by the EU for all geo-referencing in Europe.

At the moment, a part of the services and research described above and below are based on multiple GNSS, more specifically on GPS and GLONASS (Russian equivalent of GPS) observations (see figure to the right, showing the present state of the EPN). With the upcoming GALILEO positioning system, the scientists involved in this project will also work on the incorporation, processing, and enhancement of GALILEO precise positioning in the research and the services they maintain.

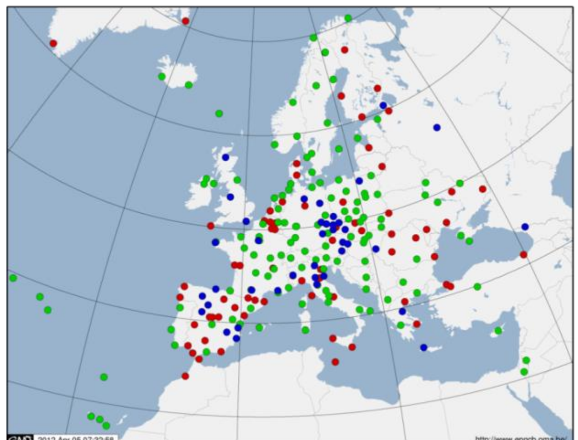

EPN tracking network (status Dec. 2011). Red: stations tracking only GPS signals (32%;) Blue: stations tracking GPS+GLONASS signals (52%); Green: stations tracking GPS+GLONASS signals and capable to track Galileo signals.

More info on the GNSS activities: www.gnss.be

In addition, based on their expertise in GNSS data processing and position determination, the team is assigned to coordinate an international working group aiming at using GNSS to determine the ground deformations at GNSS stations all over the world in a homogeneous and consistent manner so that geophysicists can use them to learn more about the Earth. Several continents have submitted results to the working group for intercomparison (see figure on top of the opposite page).

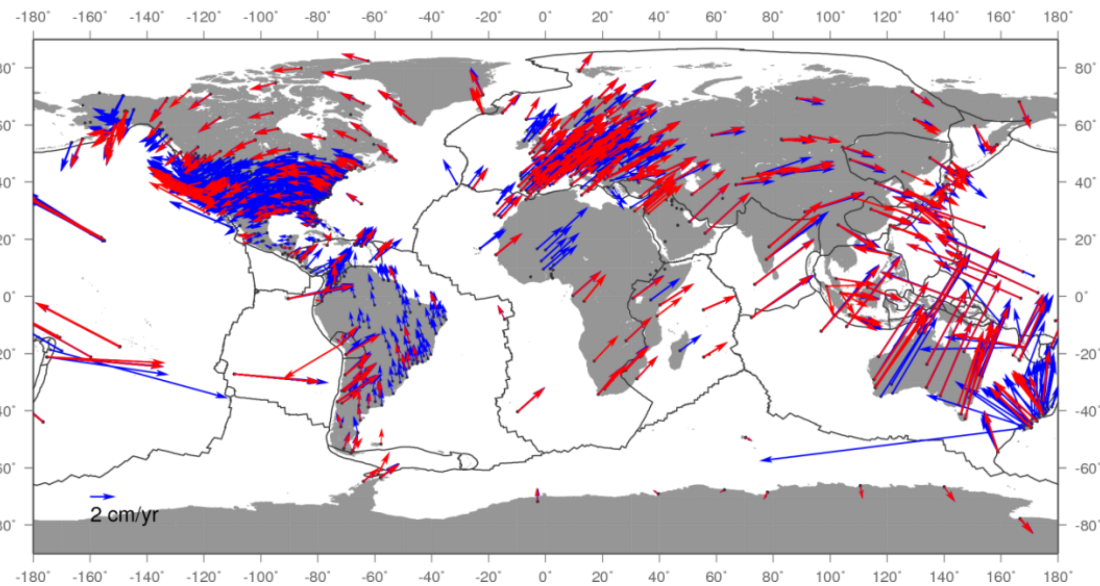

Ground deformation as measured with GNSS. In blue: velocity fields under evaluation; in red: standard velocity field available today.

The GNSS team is also involved in the Solar Terrestrial Center of Excellence (STCE) where GNSS observations are used to monitor the Earth's ionosphere and troposphere. The monitoring products are used by scientific as well as civil users. In the frame of the ionosphere, a method to generate in near-real time 0.5°x0.5° grid VTEC (Vertical Total Electron Content) maps and VTEC variance over Europe each 15 minutes from the GNSS data from the EPN has been developed (see figure below). The maps monitor the ionospheric activity and are available from the gnss.be website and have been integrated in the SIDC web portal. In addition, as it was the case in several European Agencies simultaneously involved in the EPN data analysis and performing tropospheric research, these activities found a natural synergy and led to the involvement in the EUMETNET E-GVAP (EUMETNET EIG GNSS water VApour Program) project of which the aim is to determine the water vapor content in the atmosphere from GNSS data.

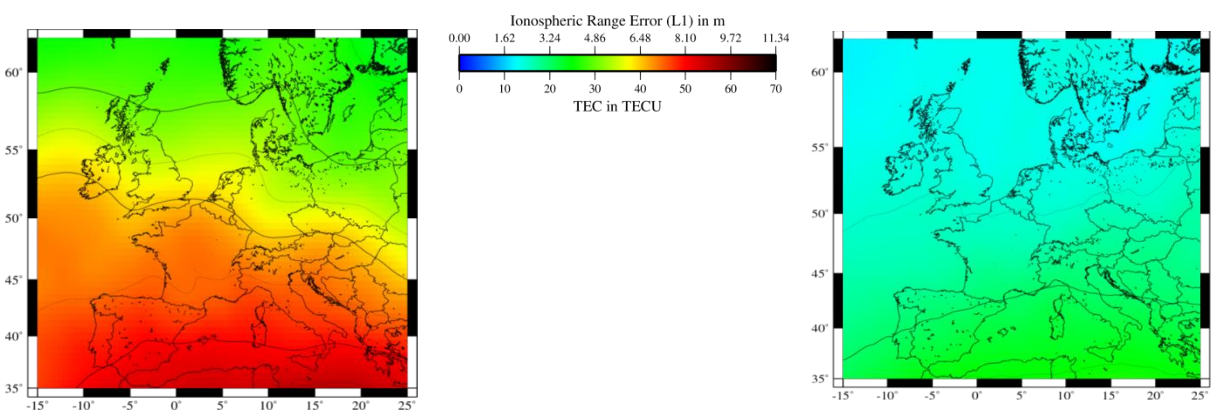

Ionospheric VTEC maps of: a) the 17/09/2011 at 13:30 UTC and
b) Median of the ionospheric activity at 13h30 over the previous 15 days (2/09/2011-16/09/2011)

The service activities described above are based on a solid dose of research that guarantees that the services are of the highest level. The research concerns the modeling, mitigation and understanding of the GNSS error sources:

The ionosphere: the team demonstrated for the first time a clear linear correlation between the 10.7 cm radio flux F10.7P monitoring solar activity and the TEC (Total Electron Content) determined from GPS. The correlations vary, at first order, with the phase of the solar cycle and, at second order, with the Earth orientation with respect to the Sun and the TEC (see figure on the right).

The troposphere: a new collaboration with the RMI and the BISA on the inter-comparison of different techniques observing the atmospheric water vapour was set up. Atmospheric water vapour is the most dominant greenhouse gas and thus important to be reliably monitored.

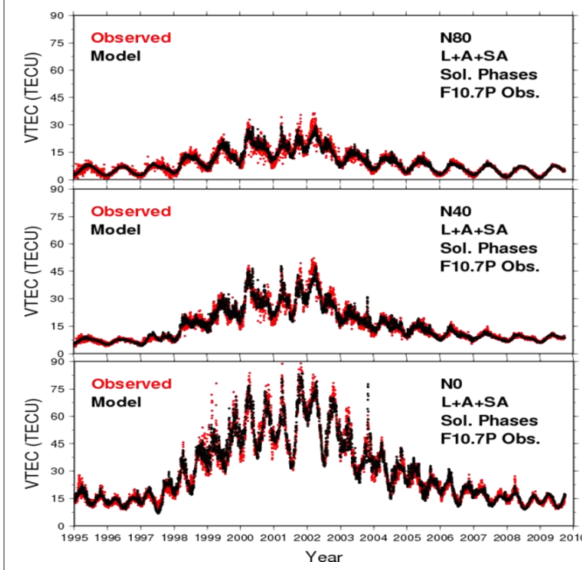

Estimated daily mean VTEC (=model in black) and observed (in red) for different geomagnetic latitudes. Bottom: geomagnetic equator. Middle: mid-latitude region. Top: polar region.

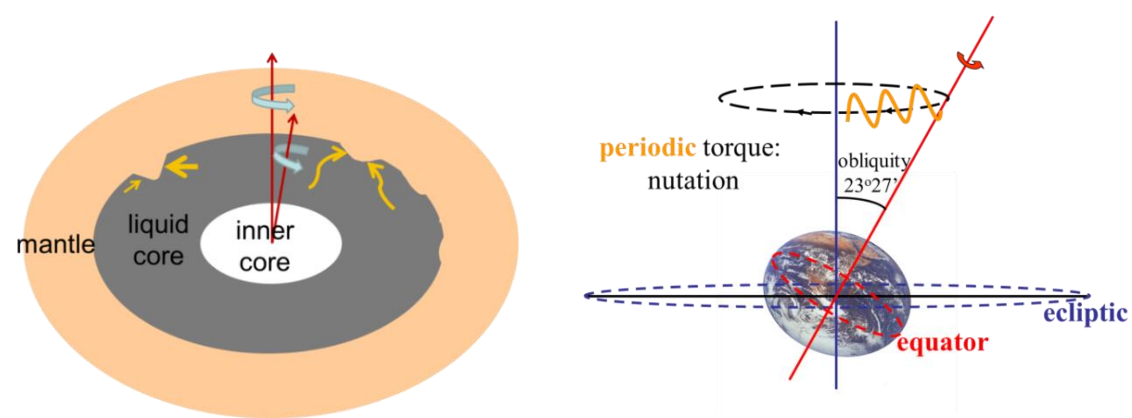

Representation of the topographic coupling at the core-mantle boundary (left). Nutation of the Earth in space (right)

Earth Rotation

The scientists working on Earth rotation have the objectives to better understand, to model the Earth rotation and orientation variations, and to study physical properties of the Earth's interior and the interaction between the solid Earth and the geophysical fluids. The work is based on theoretical developments as well as on the analysis of data from Earth rotation monitoring and general circulation models of the atmosphere, ocean, and hydrosphere. The scientists involved in this project work on the improvement of Very Long Baseline Interferometry (VLBI) and GNSS observations and on the determination of geophysical parameters from these data, as well as on analytical and numerical Earth rotation models. They study the angular momentum budget of the complex system composed of the solid Earth, the core, the atmosphere, the ocean, the cryosphere, and the hydrosphere at all timescales. This allows them to better understand the dynamics of all the components of the Earth rotation, as Length-of-day variation (LOD), polar motion (PM), and precession/nutation, as well as to improve their knowledge and understanding of the system, from the external fluid layers to the Earth deep interior (see figure on the left).

In particular, topographic coupling mechanism at the core-mantle boundary inside the Earth (and in other terrestrial planet rotating rapidly) has been computed and shown to be enhanced for particular topography wavelengths, in relation with the inertial waves excited within the liquid core. Effects on the length-of-day and on the nutations have been examined. Enhancements have been shown for particular topography features.

Electromagnetic torque at the core-mantle boundary and its effects on nutations are also studied at ROB. In particular, we have interpreted the observed frequencies and damping of free oscillations of the Earth, the so-called Free Core Nutation (FCN) and Free Inner Core Nutation (FICN) modes in terms of electromagnetic coupling at the core boundaries, of viscosity in the liquid core, and of viscous deformation of the inner core estimating the inner core viscosity, which provides new inside on the Earth interior properties (see figures below).

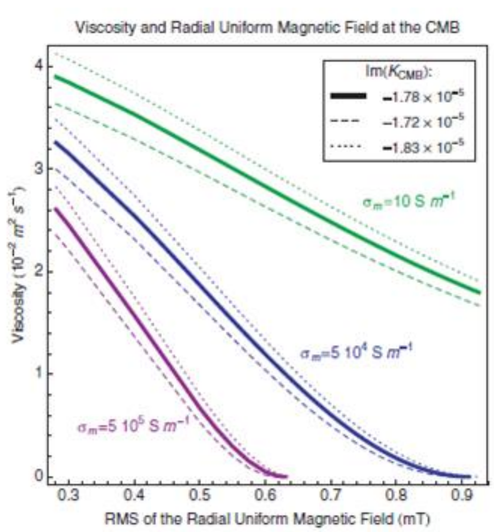

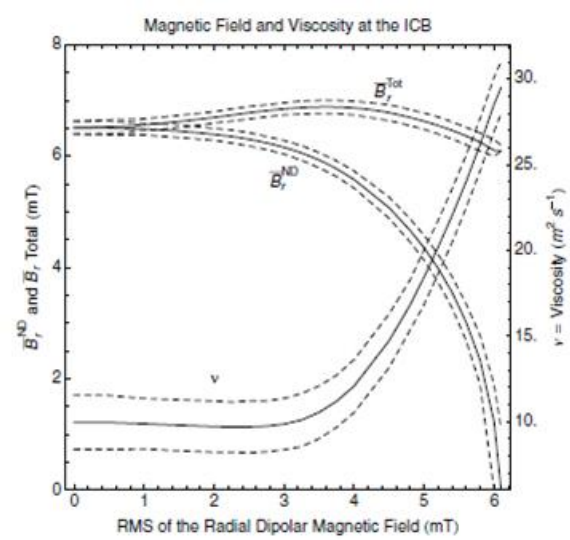

Values of the viscosity of the core and of the amplitude of the electromagnetic field determined from the coupling constant at the core-mantle boundary deduced from nutation observation, for different conductivity considered in the lower mantle.

Dipole and non-dipole electromagnetic field and viscosity satisfying the coupling constants at the inner core boundary deduced from nutation observation.

Geodesy and Geophysics of Terrestrial Planets

ROB scientists investigate the rotation and orientation variations and the tides of the terrestrial planets and large natural satellites in order to gain insight into their interior structure, composition, evolution, dynamics, and atmosphere. Geodesy data on the gravity field and rotation of a planet can be obtained from spacecraft flying by, orbiting around it, or landed on the planets. In this project, radio science data from spacecraft in orbit around Mars and Venus, such as MarsExpress (MEX), Mars Global Surveyor (MGS), Mars Odyssey, Mars Reconnaissance Orbiter (MRO), and VenusExpress (VEX) are the principal source of information. Radio science data from the upcoming BepiColombo mission to Mercury and the ExoMars mission to Mars will be processed in the future. In addition, we use data from missions to the outer solar system like Voyager 1 and 2, Galileo, and Cassini.

The gravity field of planetary bodies is obtained by monitoring the trajectory of passing or orbiting spacecraft through performing Doppler and ranging measurements on radio links between the Earth and the spacecraft. For the analysis of these radio science data and for simulations of future experiments, a numerical code (GINS/DYNAMO) is used and further developed; this code is one of only a few codes in the world that can compute accurate orbits of spacecraft from radio science data. Because the gravity field of a planet is determined by the planet's mass distribution, spatial and temporal variations in the gravity field can be used to determine physical properties of the interior and atmosphere of the planet. Since the beginning of the space age, the large-scale structure of the gravity field of planets and moons has been successfully used to determine the moment of inertia, which is a measure of the radial density distribution and an important constraint on the interior structure. More recent efforts use tides, which can also be observed through their time-

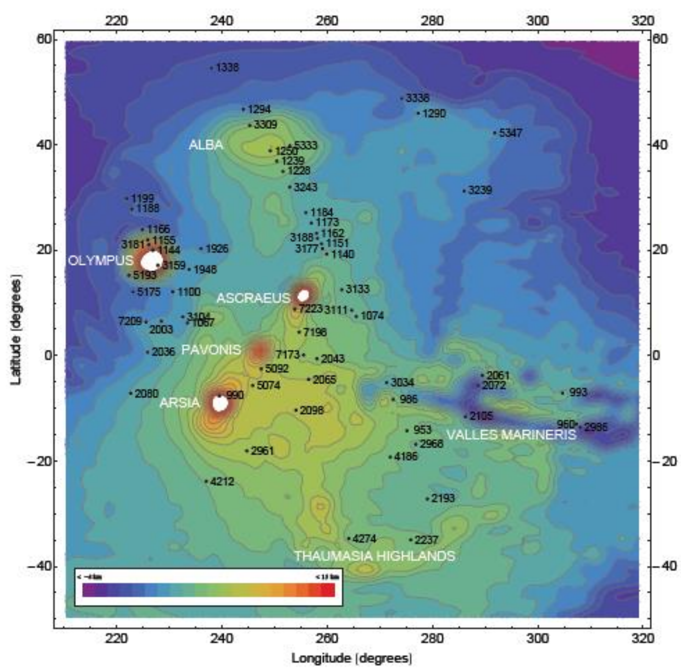

Pericenters of gravity passes with MarsExpress in the Tharsis province, superimposed on the topography

variable effect on the gravity field, to obtain more accurate information on the deep interior, in particular on global fluid layers such as a liquid iron core in terrestrial planets and an internal subsurface ocean in icy satellites.

Constraints on planetary interiors can also be obtained from rotation variations. Three broad classes of rotation variations are usually considered: rotation rate variations, orientation changes with respect to inertial space (precession and nutation), and orientation changes with respect to the rotation axis (polar motion and polar wander). They are due to both internal (angular momentum changes between solid and liquid layers) and external (gravitational torques) causes. By studying rotational variations of a terrestrial planet, more can be learnt about the excitation processes. Moreover, as the rotational response depends on the planet's structure and composition, also insight into the planetary interior can be obtained. This is particularly so for the rotational variations due to well-known external gravitational causes, such as for example for the nutations of Mars and the librations of Mercury and natural satellites.

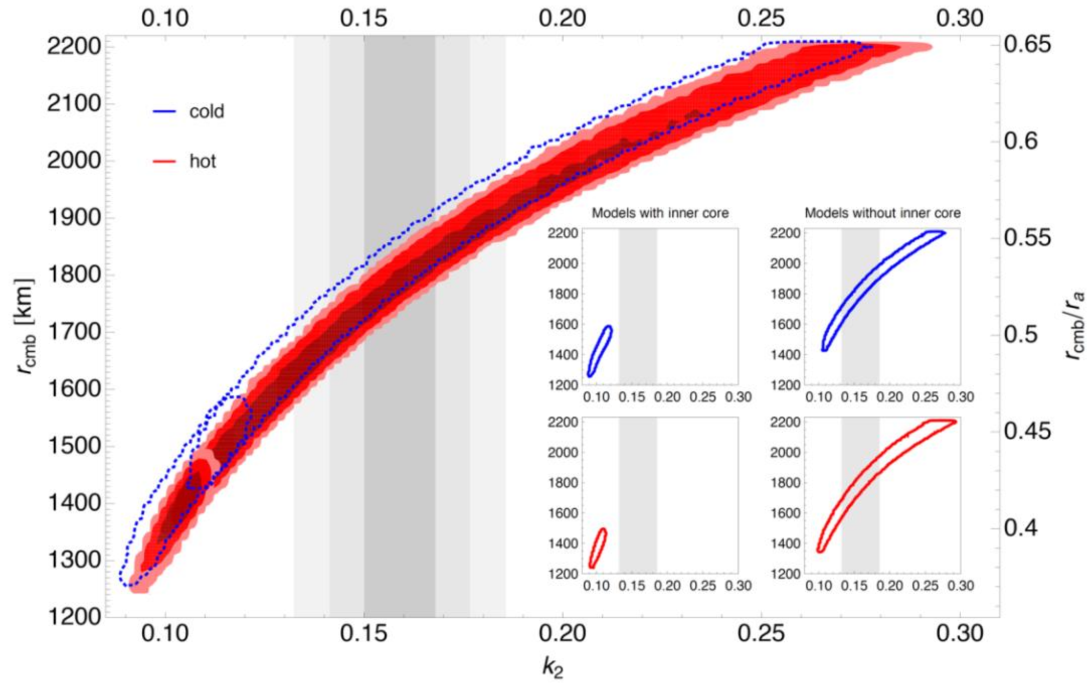

Core size as function of k_2 for the hot and cold mantle temperature for models that satisfy the moment of inertia. Contours delimit domains corresponding to 0.997, 0.954, and 0.682 probability of occurrence. The blue dotted lines delineate the 0.997 domains of the cold models. The grey shaded areas represent the k_2 values of Konopliv et al. (2011), for 1, 2, and 3 s. The insets correspond to the individual 0.997 contours of the models with an inner core and without an inner core for cold and hot mantle models.

About the planet Mars:

During several orbits, the radio science experiment MaRS aboard Mars Express acquired gravity data above the Tharsis volcanoes, which form the largest volcanic region in the solar system (see figure above). The data analysis shows that the overall density of the volcanoes is higher than the expected density of the Martian crust, in agreement with the basaltic composition of many Martian meteorites probably originating in the Tharsis area, and that one volcano, Ascraeus Mons, differs from the others in being of lower density in its upper part, though its overall density remains high.

If the Tharsis Montes were built in succession by a unique moving mantle plume, this suggests that Ascraeus Mons formed as the last of the Tharsis Montes. It was also shown that Olympus Mons, the highest mountain in the solar system, lacks a high density root, which indicates that it was built on a crust of high rigidity (or lithosphere), whereas the other volcanoes partly sunk within a less rigid lithosphere.

From the latest available data on the moment of inertia and the tidal amplitude of Mars the most accurate estimates ever have been determined on the core size and composition of Mars. It has been shown that at the 1σ confidence level the core size is expected to be in the interval [1716, 1850] km (see above) and the weight fraction of sulfur in the core is in the interval [13,18] wt%. For the current ideas about the temperature in Mars, the high sulfur estimate implies that the core of Mars is entirely liquid and contains no solid inner part, in contrast to the Earth.

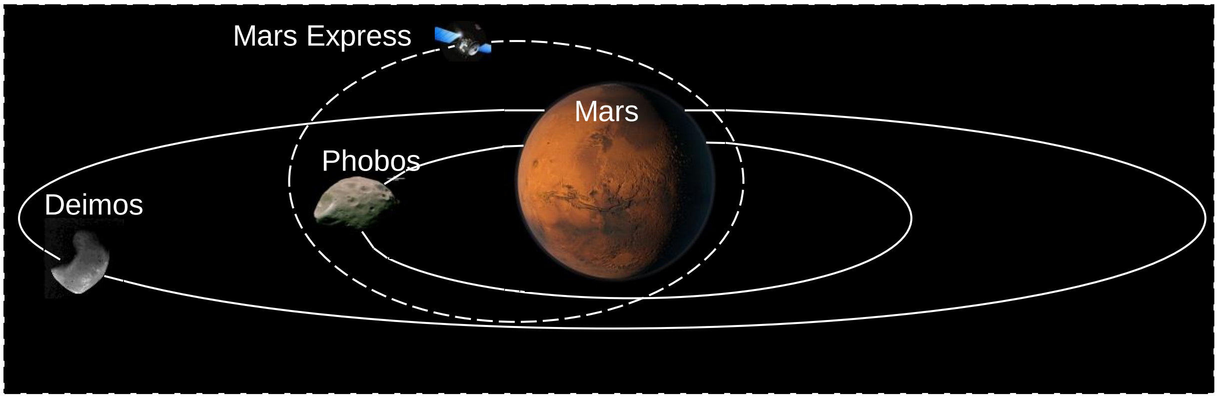

Orbit of MarsExpress, the ESA spacecraft around Mars, and of the two moons of Mars, Phobos and Deimos.

About the moon of Mars, Phobos:

The Martian moons Phobos and Deimos may be asteroids captured by Mars or they may be formed in situ from a circum-Mars debris disk. Their density is lower than any possible material analog, suggesting that they either have a high interior porosity (voids) or contain a large fraction of low-density material, most likely in the form of water ice. We have shown that precise measurements of the gravity field and the rotation variations (librations) of these bodies may help to estimate the content of water ice and hence to better understand their origin since a high (low) content in water ice would support the capture (in-situ) scenario. Phobos gravity field measurements are foreseen in the coming years by the Mars Express radio science experiment

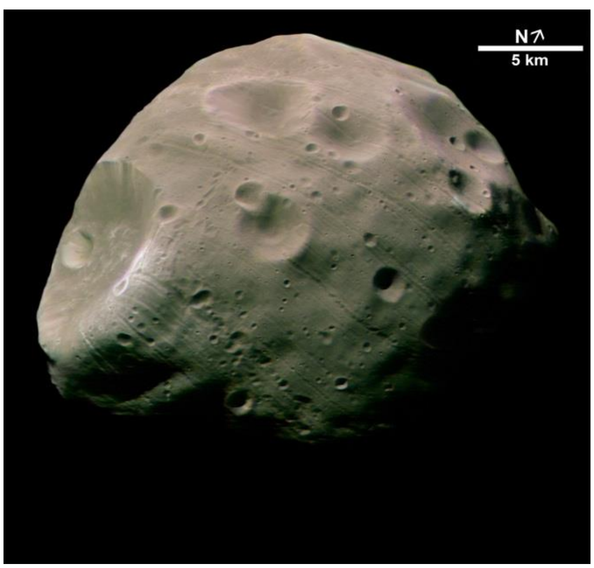

Image from MarsExpress (copyright ESA-DLR) of Phobos, the closer to Mars of the two Martian moons.

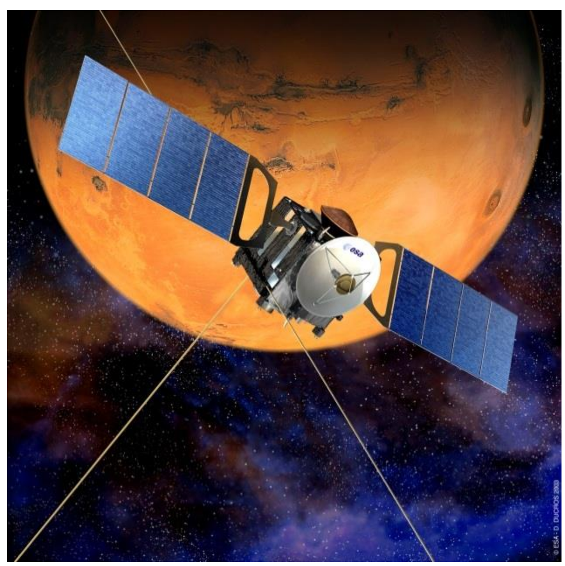

MarsExpress ESA spacecraft, presently around Mars

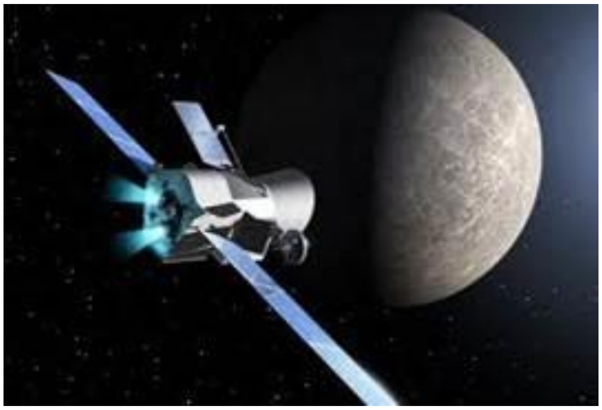

BepiColombo mission to Mercury (credit ESA)

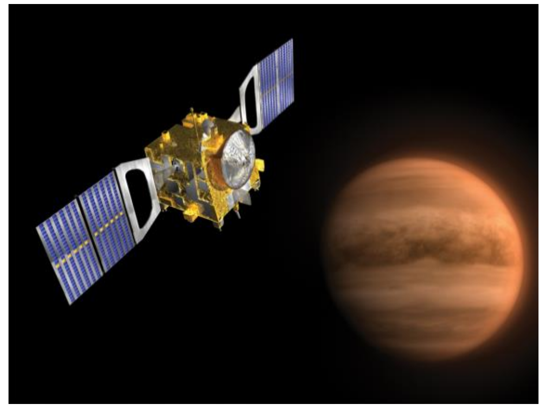

Venus Express mission (credit ESA)

About the planet Mercury

Mercury is probably the only other terrestrial planet of the solar system that like the Earth has a solid inner core in the otherwise liquid iron core. A new method to prove the existence of an inner core and to determine its size has been proposed which relies on the potential observation of a free translational mode of the inner core of Mercury. We have shown that observation of the period of the mode could be used to constrain the size of the inner core. It has also been demonstrated that an impact by a meteoroid with a radius of at least 100 m could excite the mode to a level observable by the upcoming BepiColombo mission, but that the estimated damping time of the Slichter mode is well below the average time between impacts of at least that size, requiring a recent impact (less than 0.5 My ago).

A method has been developed to study the effect of tides and an inner core on the libration of Mercury. The effect of tides is shown to be below the current and future expected observational precision, but the effect on the libration amplitude could be observed for cores larger than 1000km. An inner core also changes considerably the free libration period by up to 25% if the inner core is very large. Besides giving information on the moment of inertia of the silicate shell, observations of Mercury's libration can therefore also yield information on the inner core. In particular, libration at periods longer than the orbital period of Mercury could be the best way to obtain information on the inner core of Mercury from librations because of possible resonances with planetary forcing.

About the planet Venus

First ever measurements of the mass density of the upper thermosphere close to the north pole of Venus at minimum solar conditions have been performed when the Venus Express (VEX) spacecraft passed through that region on 14-25 October 2010 and on 23 May – 3 June 2011 at an altitude of about 165 km. The density of the atmosphere of Venus over the North Pole has been derived from measurements of the drag through VEX radio tracking and has been shown to be about half that predicted by the current models.

About the Moon

In collaboration with French planetary scientists, a new model has been proposed for magnetic field generation where dynamo action comes from impact induced changes in the Moon's rotation rate. The predicted surface magnetic field strength, on the order of several micro-Tesla, are consistent with paleomagnetic measurements of Moon rocks brought to Earth by Apollo astronauts.

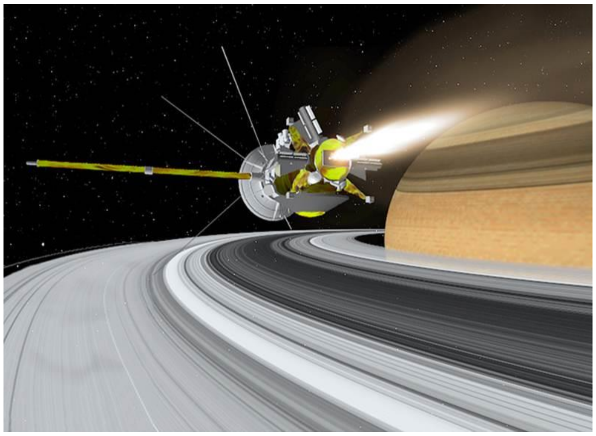

NASA-ESA Cassini-Huygens spacecraft for the observation of the Saturnian system and Titan in particular

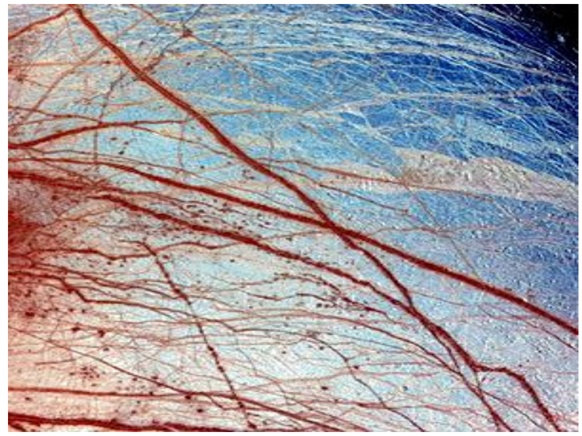

Cassini (NASA-ESA) image of the surface of Europa.

About the large natural Satellites:

The ROB planetary scientists have developed a method to study the obliquity, or angle between the rotation axis and the normal to the orbital plane, of icy satellites that have a global subsurface ocean in order to explain the difference between the observed obliquity value of 0.3 degree for Titan, the only icy moon for which the obliquity has been measured, and the much smaller previously predicted value. It has been shown that, with a subsurface ocean, theoretical obliquity values can be obtained in agreement with the observed value by the Cassini radio science team, suggesting that also Titan has a subsurface ocean.

By means of a simulation study to assess the sensitivity of Doppler measurements on radio links between an orbiter around Europa or Ganymede and the Earth to tides and rotation variations, we have shown that subsurface oceans on Europa or Ganymede can be detected through Doppler tracking of an orbiting spacecraft. The shell thickness of Europa could be estimated with an accuracy of the order of 20 km.

In general:

The team has thus a strong theoretical research component, which is oriented towards the investigation of the dependence of rotation variations, gravity field, and tidal variations on interior and atmosphere properties and orbital motion characteristics. These studies include the development of advanced models of rotation, the construction of detailed models for the structure and dynamics of solid and fluid layers of the planets, the investigation of the dynamical response of these models to both internal and external forcing, the modeling of the orbital motion of large bodies of our solar system, and the inclusion of general relativistic effects into the data analysis.

We are involved in several ESA solar system missions (Mars Express, Venus Express, BepiColombo) and Cassini at Co-Investigator level, actively participate with ESA in preparations for new and upcoming missions (e.g. the candidate L-class mission to the Jupiter system, JUICE), and lead the development of a coherent X-band transponder and antenna for use in a future Mars lander mission. We also develop theories and strategies for the future exploitation of space data

Time – Time Transfer

The ROB scientists establish the Belgian time scale (UTC(ORB)) and participate in international timescales by incorporating Belgium in these timescales. We maintain presently six high-quality clocks for participation in two international timescales: the International Atomic Time (TAI) and the International GNSS Service Timescale (IGST). The present requirement for the clock precision and stability is at the level of the nanosecond over one day, which can only be achieved with high-quality clocks, when located in temperature-controlled environment. Our six clocks are located in such an environment and their performances are continuously monitored by inter-comparison between themselves and also with atomic clocks of other laboratories participating to TAI or IGST. In order to perform these comparisons, as well as to transfer time at the centers where the computations for the international timescales are performed, we need methods which ensure a time-transfer precision matching the required precision of the timescales. These comparisons are usually performed using code measurements of GPS satellites in common view. The scientists involved in the project work on the improvement of the time transfer by using both code and phase measurements of geodetic receivers, in order to enhance its precision and accuracy. This requires the establishment of new analysis strategies, new error modeling, and new computer codes. It also requires the installation of new equipment and the adaptation of the procedures to these new equipment. The scientists of this project also take care of the legal issues related to the legal time. An additional important part of the work is related to the quality control and maintenance of the clocks, as our involvement in the definition of international timescale impose us a quasi-perfect reliability.

During the year 2011, the ROB Precise Timing Facility (PTF or time laboratory) was completely renewed, with three new cesium beam atomic clocks and a new time delay generator providing a more robust generation of UTC(ORB). The PTF is also equipped with an active control and monitoring of all the active clocks, allowing a real time detection of anomalies. The top right figure provides the difference between the realization of UTC at ROB and UTC as a function of time for 2011.

With the up-coming Galileo, ROB scientists have evaluated the performance of time transfer based on the new-defined signal (ionosphere-free combination of Galileo E5 code-plus-carrier (CPC) combination) and have demonstrated that this provides a noise level 10 times lower than other ionosphere-free combination while medium-and long-term stability of time transfer is not improved. See bottom right figure.

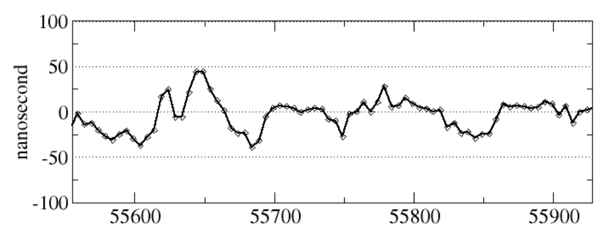

UTC(ORB) compared to the true UTC during the year 2011.

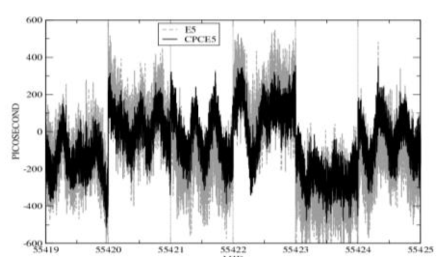

Differences between the simulated clock and the computed clock obtained with either E5 code directly or the E5-CPC combination.

Gravimetry & Seismology

Composite Seismogenic Source Model in the Valley Rift System

In the frame of the EC project SHARE ("Seismic Hazard Harmonization in Europe"), ROB coordinates the collection of regional data for Central and Western Europe on active faults. In this framework, we conducted a more detailed study of the most active tectonic structure in our regions, the Roer Valley Rift System (RVRS). This source model provides a solid and fully documented basis for more detailed, fault-based seismic hazard assessment, and diverse modeling exercises, e.g. concerning seismic activity, crustal deformation, stress transfer and fault interaction. It also serves as a guide for further paleoseismic studies, showing where more studies are needed to better determine seismogenic parameters.

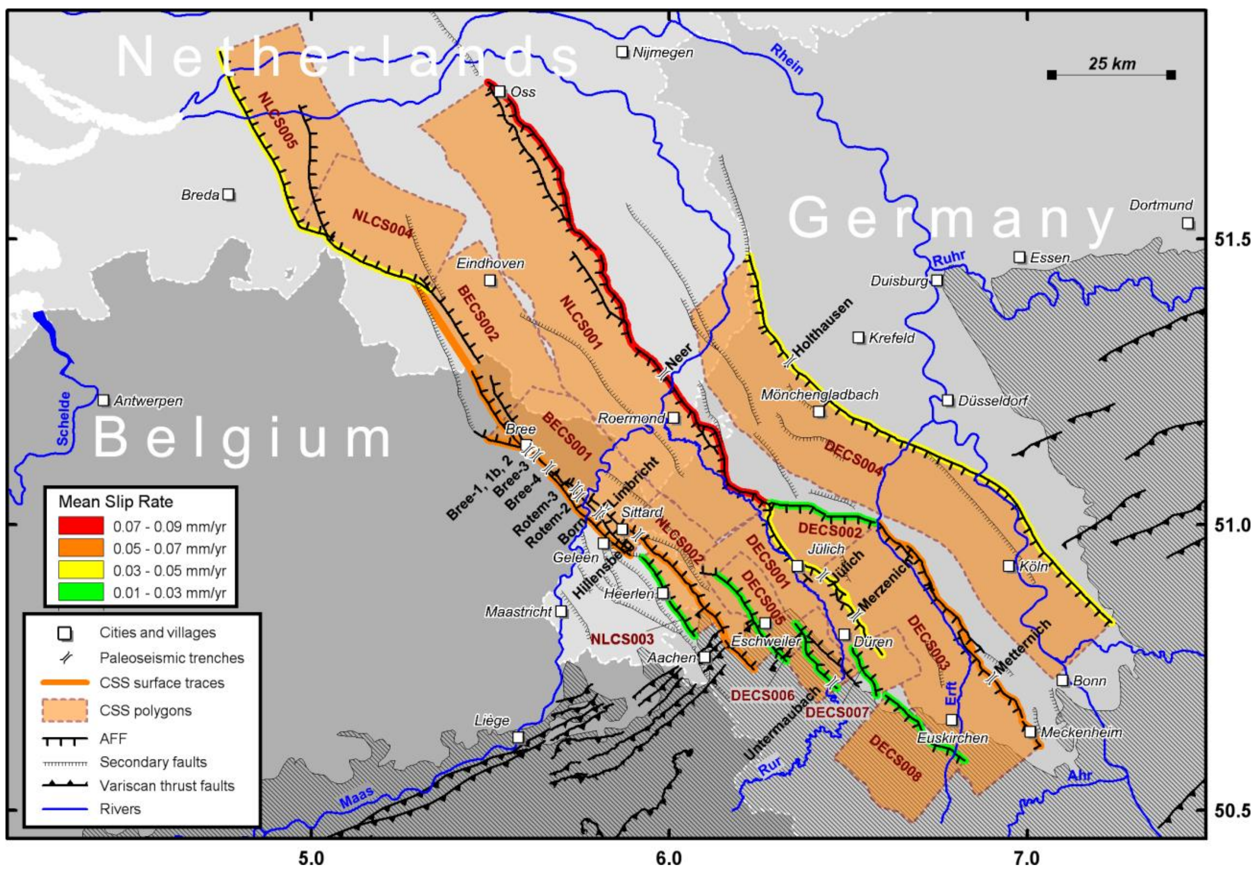

Model of seismic sources in the Roer Valley Rift System. The surface traces are colored according to their slip rate.

Crustal Structure at the Princess Elisabeth Base in Antarctica

More than 300 teleseismic (epicentral distance > 30°) earthquakes (red crosses) were recorded at our seismic station ELIB, installed since 2010 at the Princess Elisabeth Base in Antarctica. Among these events dataset, 38 were selected (blue crosses) for computation of receiver functions allowing a first estimate of the crustal thickness in this part of Antarctica.

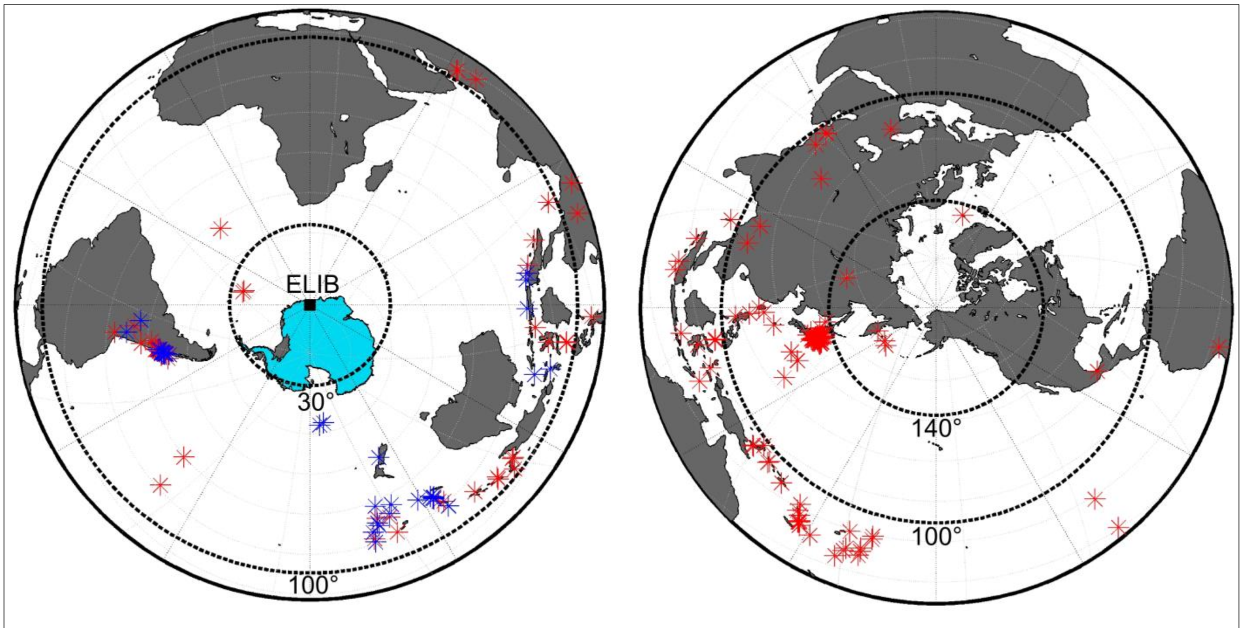

Map of the earthquakes' epicenters

By enhancing P-wave to S-wave conversions, this technique allows to determine depth and characteristics of the major discontinuities inside the Earth such as the Moho, the limit between the crust and the mantle. The stack of individual RF (bottom right figure) shows clear P-to-S signal from the Moho discontinuities at 5.7 sec, inferring a Moho depth at 44 – 50 km.

This Moho depth value suggests the presence of an orogenic crustal root beneath the region and may be related to the amalgamation of Antarctica and Africa into the Gondwana supercontinent about 600-500 million years ago.

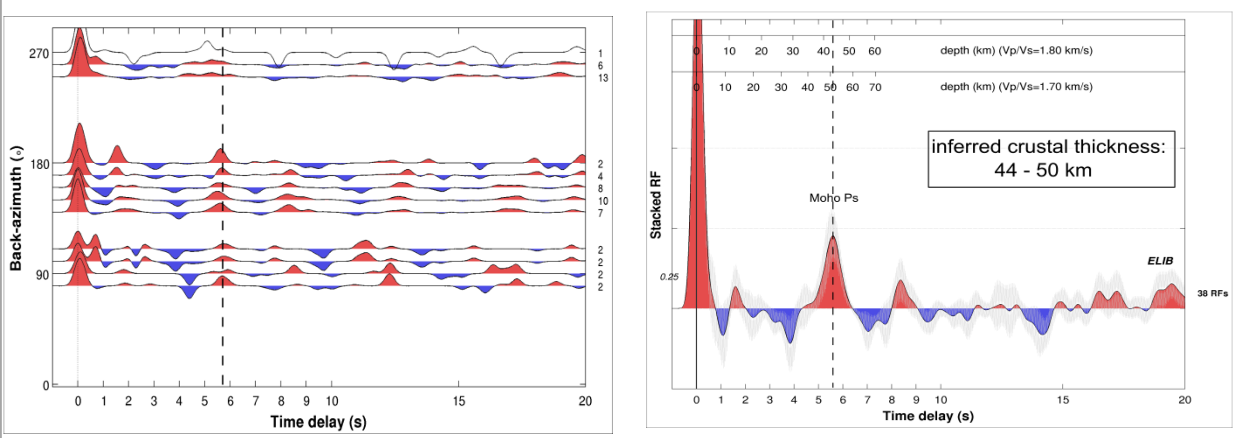

Left: discontinuities; Right: stack of individual RF with a clear signal from the Moho

The volcanic hydrothermal system of Kawah Ijen in Indonesia

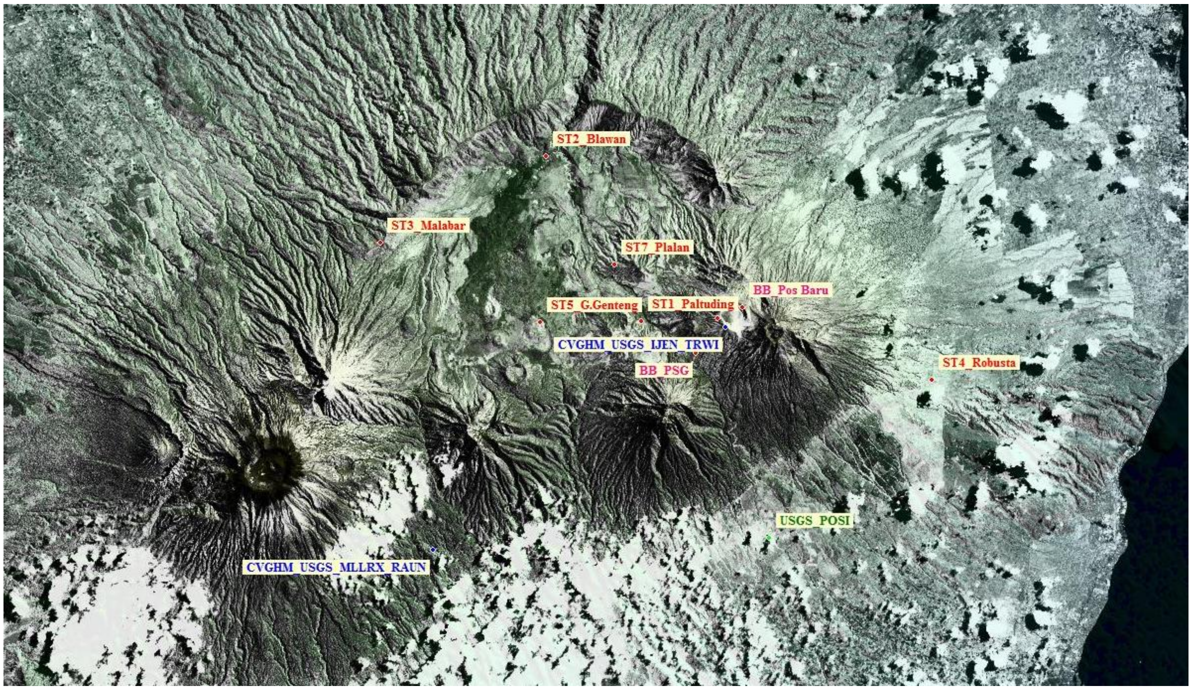

Kawah Ijen seismic network (Blue and Green: USGS and CVGHM seismic stations / Red and pink: ROB seismic stations, respectively short period and broadband sensors)

Since June 2010, we equipped the Kawah Ijen volcano with broadband and short-period seismometers, but also with temperature and level instruments which have been immerged into the largest acidic lake in the world. About 2000 seismic events have been recorded and analyzed. The study of the noise wave field and its cross-correlation improved the understanding of the volcanic crisis that occurred in May 2011 and December 2011. Our monitoring techniques have been implemented to the daily monitoring of the volcano.

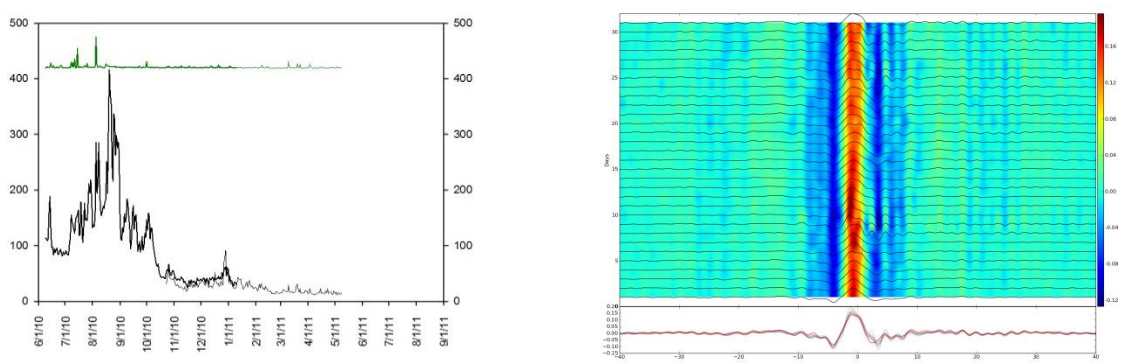

Left: Evolution of the amplitude of the seismic noise between June 2010 and May 2011 in the 2-4 Hz frequency band (black curve: mean amplitude / green curve: standard deviation of the amplitude) / Right: Cross Correlation function shifted during the first days of unrest, in July 2010. It suggests a change of velocity in the upper part of the crust which correlates with high amplitude in the 2-4 Hz frequency band.

The Seismic Alert System

Since March 2010, we host the common web-based macroseismic questionnaire for the ROB and the Seismology Section of the University of Cologne. In 2011, two earthquakes were strongly felt in Germany, the Netherlands and Belgium and the macroseismic data flowing in real time allowed both institutes to inform their authorities efficiently. The alert system linked to the inquiry also worked as expected for all felt events in and around Belgium. We also improved the availability of the information for the seismologists by refactoring the “alert” website and the emails sent when events are detected by SeisComp3, the automated earthquake detection and location package. The emails and website now provide maps and seismograms to ease the understanding of the messages. The website has also been structured to be readable and accessible from a smartphone. The current system allows warning the authorities of a felt earthquake within 10 minutes after its occurrence, already providing important information about its impact on the population.

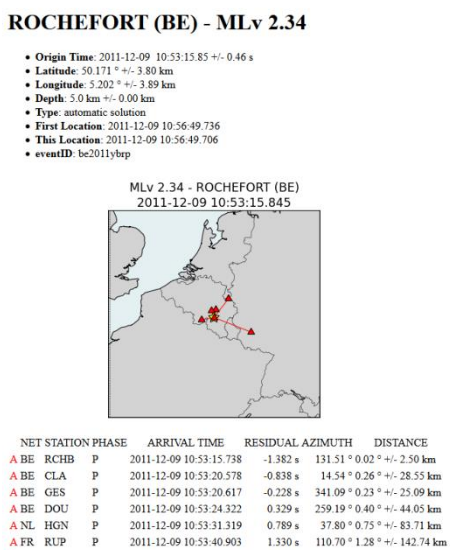

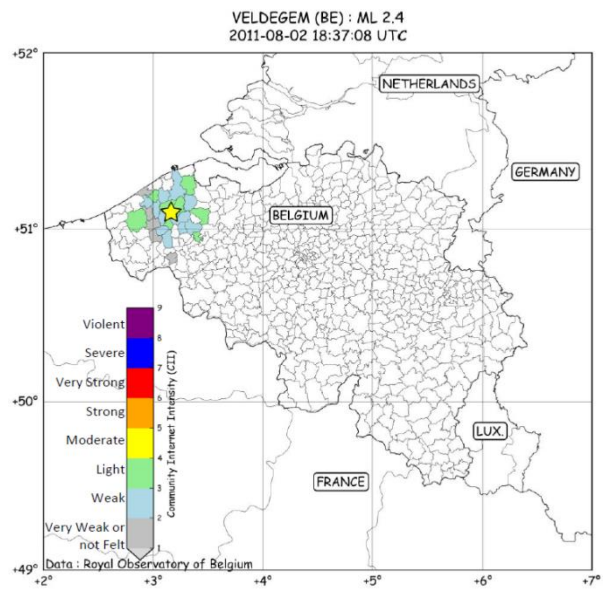

Example of an alert sent by email for a detected quarry blast near Rochefort (BE) & Example of a macroseismic intensity map produced for the M_L=2.5 Veldegem Earthquake (2 August 2011).

Absolute Gravity measurements to measure deformation of the Lithosphere in Northwest Europe

In northwest Europe, ground surface movements are close to or below the accuracy of current geodetic techniques. Our goals are to investigate the relative contributions of the tectonic forces, climatic loading (e.g. glacial isostatic adjustment (GIA) and slow climate changes) and anthropogenic effects.
An absolute gravimeter is valuable to quantify slow vertical movements, as this instrument does not depend on any terrestrial reference frame. Repeated absolute gravity (AG) measurements have been performed in Oostende (Belgian coastline) and at 8 stations along a southwest-northeast profile across the Belgian Ardennes and the Roer Valley Graben (Germany).

After 9-16 years (depending on the station), all stations but Jülich show that the rates of change of gravity fall in the [-2.4, 7.3] nm/s²/yr interval. At all stations but Jülich, the results agree, within the error bars, with the subsidence predicted by the GIA (figure below). At 5 stations in the profile (Bensberg, Monschau, Membach, Sprimont and Manhay) and in Oostende, the gravity rates of change do not significantly differ from zero. Significant increases lying in the 0.2-7.3 nm/s²/yr interval are found in the two southernmost stations Werpin and Sohier. For Jülich, where anthropogenic subsidence takes place, combining this residual gravity rate of change with the vertical velocity (13.6 mm/yr) provided by repeated leveling, indicates an increase in density caused by compaction processes.
After correcting for the GIA effect, the inferred vertical land movements reduce to zero within the uncertainty level at all stations except Jülich and Sohier. The velocities as a function of longitude and latitude may indicate a possible shoulder uplift in response to rifting in the Roer Graben, but the measurements are still not precise enough to support this hypothesis. On the other hand, about 10^9 tons of water and coal have been withdrawn from the Rhur and Rur areas yearly since 1960, which is equivalent to a rate of 10^6 t/km²/yr, to be compared with the rates of 10^5 t/km²/yr due to present ice losses in Greenland or the 10^9 t/km² ice loss which occurred at the end of the last Ice Age. Due to these mass removals, the mining area might be uplifting, which may bias the results in Monschau, Membach and Bensberg, masking the GIA effect, but this cannot be resolved at this time. This illustrates the challenge to resolve very slow tectonic motions in industrialized areas.

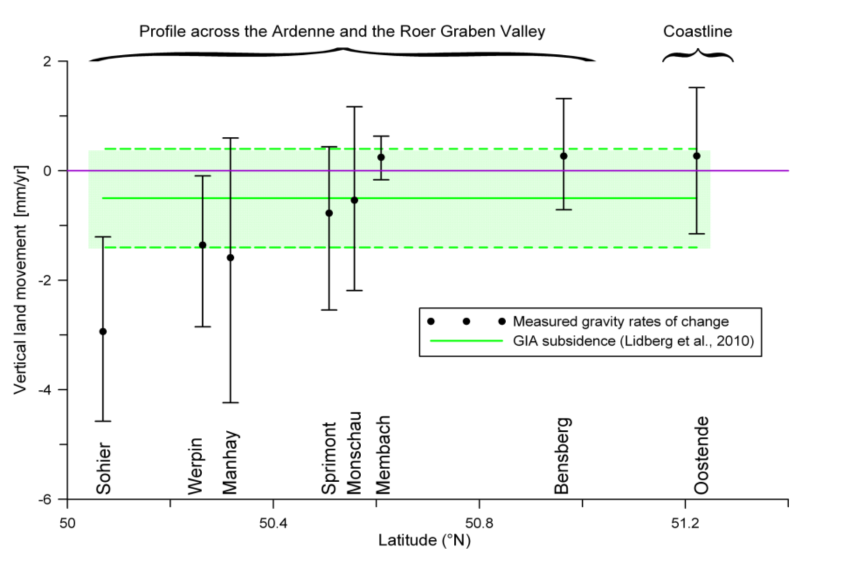

Observed velocities after applying the ratio of -2.0 nm/s²/mm on the observed gravity rates of change. The GIA predicted subsidence rate of -0.5 mm/yr is in green, with the errors bars given by the green zone. All the error bars are at the 2σ level.

Astronomy & Astrophysics

Stellar Astrophysics: Asteroseismology

The objective of asteroseismology is to probe the internal structure of (pulsating) stars. To this aim the light and spectral variations of pulsating stars are observed over a time-scale of several seasons and/or years. At the ROB we also aim at investigating the interactions that may arise between stellar pulsations and various other phenomena such as multiplicity, chemical composition and magnetic fields. As data from space missions (CoRoT, Kepler) are being distributed at a high rate, the team is becoming strongly involved in their exploitation while also participating in projects of ground-based follow-up.

An artist's impression of the COROT satellite. Credits: CNES 2006 - D. Ducros)

The CoRoT mission has provided photometric data of unprecedented quality and time-coverage also for a number of O-type stars. The analysis of the CoRoT observations of these O stars, with the star HD 46150 as main object, was finalised in 2011. The six O-type stars observed by CoRoT show diverse origins of variability: β Cep type pulsations, solar-like oscillations, the effect of rotation, the binary period and tidally induced non-radial pulsations, as well as red noise.

The KEPLER satellite continuously monitors over 100 000 stars. The mission is designed to search for extra-solar planetary systems using the transit technique, but the stellar data obtained are also excellent for variable star detection and asteroseismic studies. The contribution of the ROB is here in the characterisation and classification of preselected sets of variable stars in order to obtain information on the classes of variable stars as a whole and to identify interesting objects for further study. A study of the A-F type stars led to a sample of 750 candidate variables and will be used to investigate the relation between γ Doradus (γ Dor), δ Scuti (δ Sct), and hybrid stars. The analysis of the B-type stars was also finalised in 2011 and published.

Credit: NASA/Kepler mission/Wendy Stenzel

Spectroscopic observations were used in the analysis of two Kepler targets for which papers appeared in 2011 in the prestigious journals Nature and Science:

- KIC7548479: a δ Scuti star showing clear evidence for the simultaneous presence of p-mode oscillations excited by the opacity mechanism and stochastically driven solar-like oscillations.

• HD181068: a red giant in a triply-eclipsing compact hierarchical triple system for which evidence of tidally-induced oscillations driven by the orbital motion of the close pair is found.

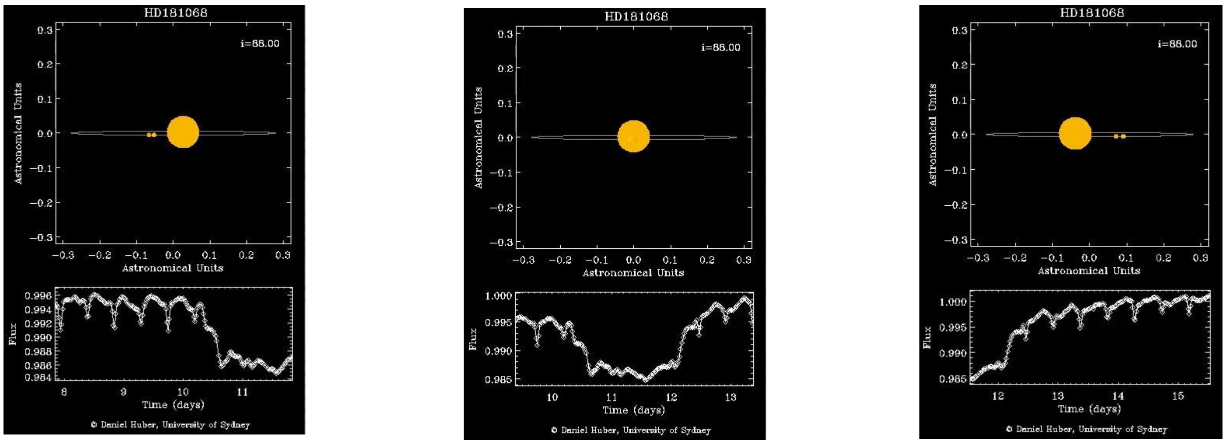

Kepler-band light curve of HD 181068 and simulation. The minimum of the 45.5-day eclipse and the minima of the 0.9-day eclipses are visible. (© Daniel Huber, University of Sydney)

Special attention is given to the study of **pulsating components of binary or multiple stars** in order to improve our knowledge of pulsation physics through constraints on the physical parameters of the pulsating component derived from the binary or multiple nature of the system, and to study the interaction between pulsation and binarity.

An intensive study was done on the bright star θ^2 Tauri. This is an interferometric-spectroscopic binary system and the brightest member of the Hyades cluster whose components also show a complex pattern of pulsations of type δ Scuti. Due to the fast rotation of the components, mainly of the secondary, the lines in the observed composite spectra are heavily blended. The analysis of Echelle spectra using the spectra disentangling algorithm led to a new spectroscopic orbit for this difficult system. The orbital parallax and the component masses were obtained with unprecedented accuracy, combining both spectroscopy and long-baseline optical interferometry. Echelle spectra obtained with the new HERMES spectrograph mounted at the Mercator telescope were also used in this study.

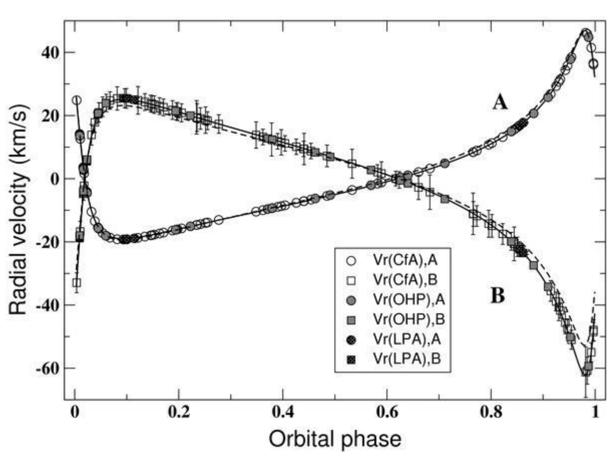

Orbital solution for the spectroscopic binary star θ^2 Tauri plotted with component radial velocities. The data are from the Oak Ridge Echelle Spectrograph (Harvard-Smithsonian Center for Astrophysics,CfA, the Elodie spectrograph (Observatoire de Haute-Provence, OHP) and the Hermes spectrograph (Mercator telescope, Roque de Los Muchachos Observatory, LPA).

Gaia: The Billion Star Surveyor

Gaia is an ambitious ESA mission to chart a three-dimensional map of our Galaxy. Gaia will provide unprecedented positional and radial velocity measurements with the accuracies needed to produce a stereoscopic and kinematic census of about one billion stars in our Galaxy and throughout the Local Group. This amounts to about 1 per cent of the Galactic stellar population. Combined with astrophysical information for each star, provided by on-board multi-colour photometry, these data will have the precision necessary to quantify the early formation, and subsequent dynamical, chemical and star formation evolution of the Galaxy. Additional scientific products include detection and orbital classification of extra-solar planetary systems, a comprehensive survey of objects ranging from huge numbers of minor bodies in our Solar System, large numbers of variable objects, through galaxies in the nearby Universe and distant quasars. It will also provide a number of stringent new tests of general relativity and cosmology.

Gaia Deployable Sunshield Assembly (DSA) in 2011 fully deployed at Astrium Toulouse (copyright Astrium)

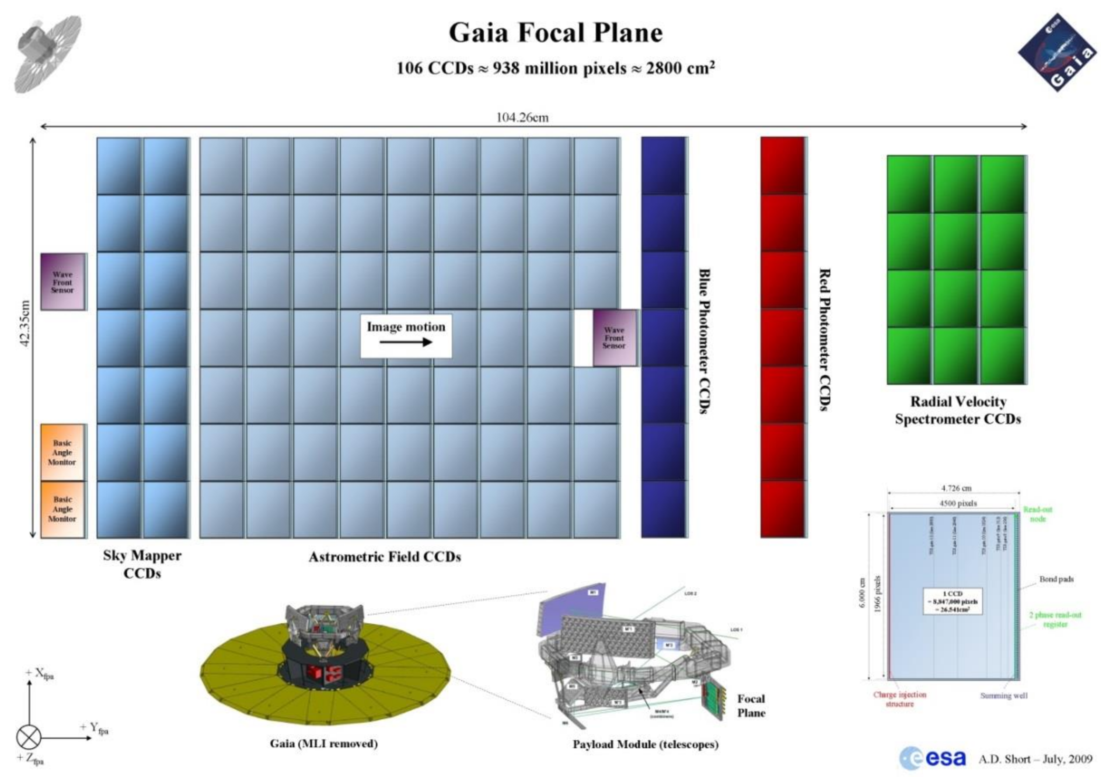

The Gaia focal plane will be the largest ever developed, with 106 CCDs, a total of almost 1 Gigapixels and physical dimensions of 0.5m × 1m (Image credit: ESA - A. Short)

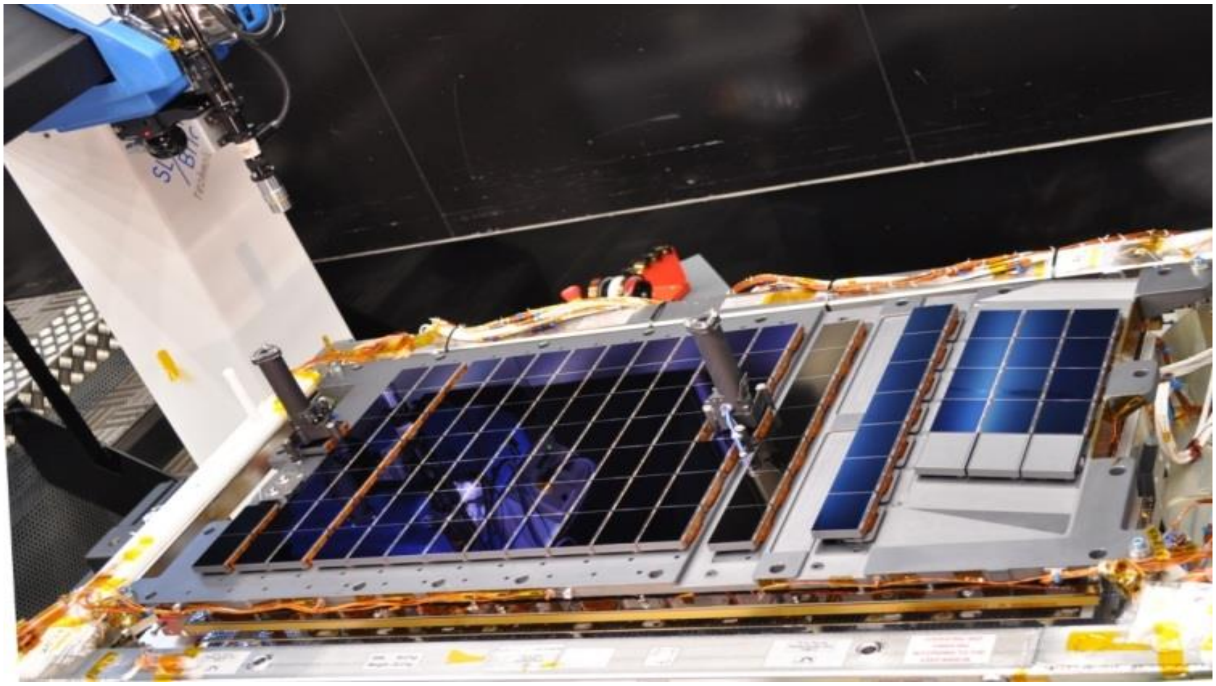

The complete set of 106 CCDs that make up Gaia's focal plane was assembled in 2011 (Copyright: ESA/Astrium)

The ROB astronomers and co-workers contribute in different disciplines to the software development of the Gaia data reduction. This data reduction has been assigned to DPAC (Data Processing and Analysis Consortium). Inside DPAC several Coordination Units (CUs) were created. In CU4 (Object Processing) the ROB is involved in the Astrometric Reduction of Solar System Objects. For CU6 (Spectroscopic Processing) ROB has the responsibility to develop different techniques that will allow measuring the radial velocities of the stars. The characterization of variable objects, with emphasis on period search of variable stars is the main contribution of ROB to CU7 (Variability Processing). Within CU8 (Astrophysical Parameters) ROB develops algorithms and codes for the calculation of astrophysical parameters for extreme stars ("Cool stars", "Ultra Cool stars", "Anomalous Abundance Stars", "Emission Line stars" and "Hot Stars").

In 2011 all ROB collaborators send new and improved versions of their Gaia codes to the data processing centers of the CUs. They contributed substantially to the documents and reports on the mission and assisted at the semestrial international meetings of the CUs.

ROB is also involved in the Gaia-ESO Public Survey. This survey has been awarded 300 nights (over 5 years) on the VLT-FLAMES instrument at the Paranal site of ESO. The observations started at the end of 2011.

Late evolution phases and mass loss

Essentially all stars with an initial mass between 1 (as our Sun) and 8 solar masses will pass through the Asymptotic Giant Branch (AGB) phase at the end of their life before becoming planetary nebulae (PN) and white dwarfs. Mass loss is one of the main characteristics of AGB stars and a main research topic of the astrophysicists of the ROB. Because of the nucleosynthesis that takes place in the interior and the dredge-up of the processed material to the surface, AGB stars, together with possibly supernovae, dominate the return of gas from stars to the interstellar medium (ISM) from which new generations of stars are born. The central stars are cool (Teff < 3000 K) and since dust usually forms close to the star, AGB stars are also very important contributors to the dust content in the ISM.
The study of AGB stars is manifold, but concentrates on the understanding of the mass-loss mechanism, the derivation of mass-loss rates and its relation to fundamental stellar parameters, and the global evolution of stars on the AGB as a function of time, metallicity, mass, etc. The studies encompass sometimes individual stars or samples of stars, both in our Galaxy and in the Local Group, and sometimes more theoretical population studies to put the AGB phase in the broader context of stellar evolution.

MESS: Mass-loss of Evolved StarS

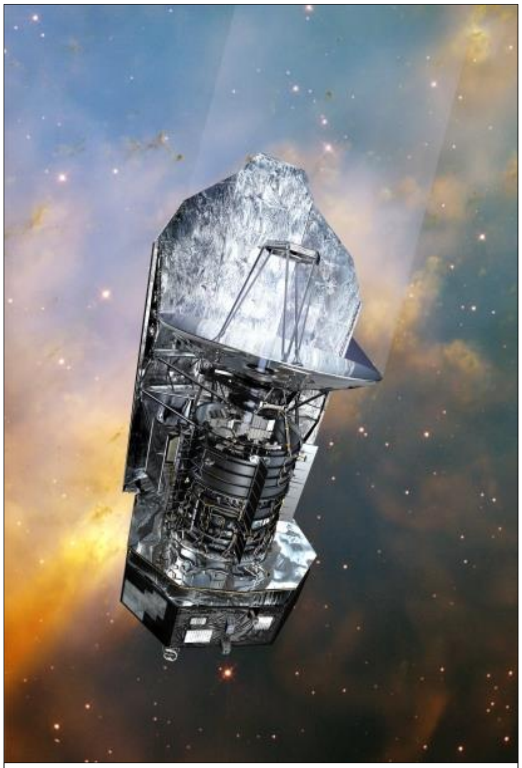

Credits Herschel/ ESA / AOES Medialab ; background: HST, NASA/ ESA/ STSc

The Herschel Space Observatory was successfully launched on May 14, 2009 and is the largest infrared space observatory launched to date. Equipped with a 3.5 metre diameter reflecting telescope and instruments cooled to close to absolute zero, Herschel observes at wavelengths in the infrared that have never previously been explored.
The ROB is leading the Herschel Guaranteed Time Key Project “MESS” (Mass loss of Evolved StarS, GTKP MESS) which brings together an international consortium of astrophysicists. In this project a wide variety of evolved stellar objects is observed in spectroscopic and photometric mode in the far-IR using both the PACS (Photodetector Array Camera and Spectrometer) and SPIRE (Spectral and Photometric Imaging Receiver) instruments on board the Herschel satellite. The main aims of this project are three-fold:
(1) To study the time-dependence of the mass loss process, via a search for shells around a wide range of evolved objects, in order to quantify the total amount of mass lost at the various evolutionary stages of low to high-mass stars,
(2) To study the dust and gas chemistry as a function of progenitor mass,
(3) To study the properties and asymmetries of a representative sample of low- and intermediate- (i.e. AGB, post-AGB, PN) as well as high-mass post main sequence objects, and supernovae.

Image of planetary nebula M76 (www.princeton.edu/~rvdb/images/NJP/m76.html) taken by Robert J. Vanderbei. (CC-BY-2.5; Released under the GNU Free Documentation License).

In 2011 the first analysis of the Herschel observations of the planetary nebula NGC 650 (also known as Messier 76 or Little Dumbbell nebula) was done. Temperature maps were constructed and analysed

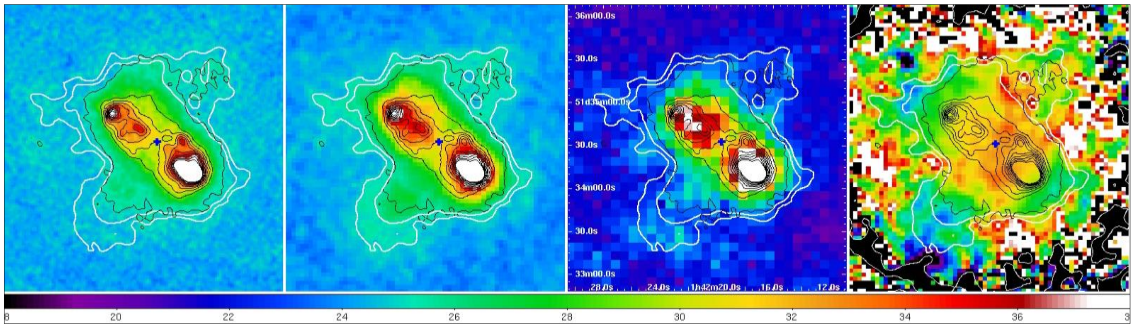

NGC 650, from left to right: PACS 70 and 160 μm, SPIRE~250 μm and the temperature map created from the PACS 70/160 μm ratio image. The black contours are of the PACS 70 μm inner region and the white contours of the fainter outer regions of the PACS 160 μm image. The blue cross marks the central star. The bar at the bottom shows the temperature scale.

We also contributed to the analysis the PACS images of the pulsating red giant star Mira. Mira's IR environment appears to be shaped by the complex interaction of Mira's wind with its companion, the bipolar jet, and the ISM.

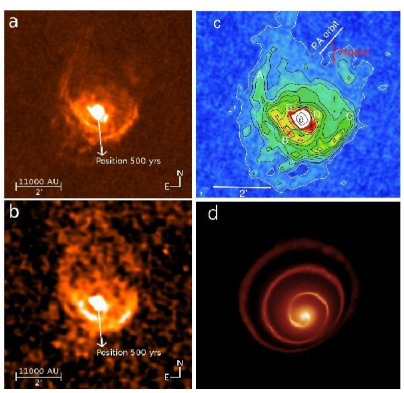

Herschel's view into Mira's head
(Mayer et al., 2011, A&A)
Panel a) deconvolved PACS image at 70 µm. The arrow indicates the space motion and the position in 500 yrs;
Panel b) is the same for the 160 µm band and
Panel c) is the 70 µm deconvolved PACS image
Panel d) results from the "toy model" based on the hydrodynamical simulations of Mohamed & Podsiadlowski (2007, 2011).

Also in other stars (X Her and TX Psc) the interaction of the stellar wind with the ISM was observed. There was also a contribution to the discovery of multiple-shells around the C-star CW Leonis. It was argued that the origin of the shells is related to non-isotropic mass-loss events and clumpy dust formation.

Herschel image of CW Leonis
This colour-composite image of CW Leonis, also known as IRC +10216, was obtained with the SPIRE and PACS instruments on the Herschel Space Observatory. It combines observations at wavelengths of 160 µm (blue; PACS), 250 µm (green; SPIRE) and 350 µm (red; SPIRE). A bow shock, created by the interaction of the stellar wind emitted by the star and the interstellar medium, can be seen to the left of the star.
Copyright: ESA/PACS/SPIRE/MESS Consortia

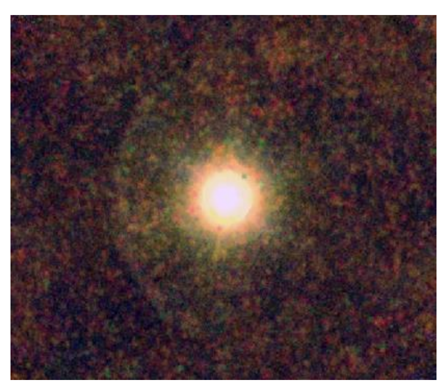

Solar Physics and Space Weather

3D Stereo Work & Linking in-situ with Remote Sensing

The majority of images and data of our Sun and the interposing interplanetary space are taken from the Earth and satellites near Earth. However, in October 2006 NASA launched the STEREO (Solar TErrestrial RElations Observatory) satellites to observe the Sun from different perspectives. STEREO consists of two satellites, with one positioned ahead of Earth in its orbit and the other trailing behind. The position of the satellites provides two new viewpoints of the Sun and its related activity, allowing solar scientists to see the structure and evolution of the Sun in greater detail and create 3D reconstructions of its features.

Each STEREO satellite houses several imaging instruments which include EUV imagers for observing the solar disk in the extreme ultraviolet wavelengths, coronagraph imagers which essentially block the Sun to allow observations of the faint interplanetary space surrounding the sun and Heliospheric imagers which observe the space between the Sun and the Earth.

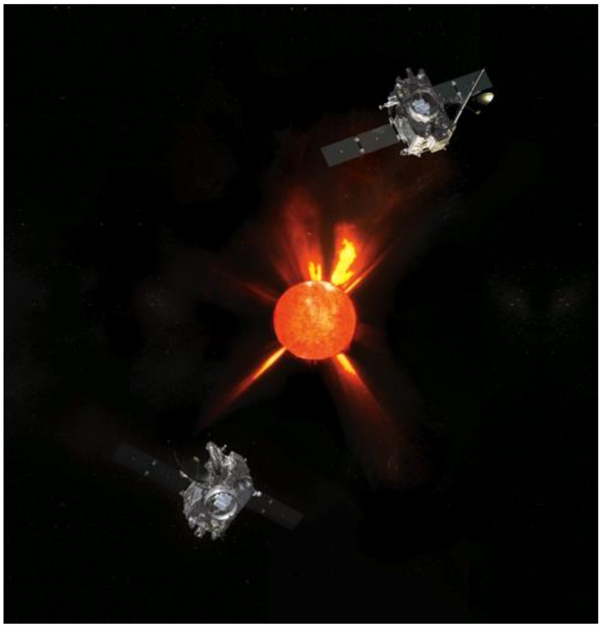

Artists view of the STEREO (Solar TErrestrial RElations Observatory) satellites observing the Sun (Credits NASA).

In recent years an important area of research in the field solar and space physics has been the study of space weather, which looks at how hot material (plasma) produced by the Sun moves out through the solar system (interplanetary space). There is a continual flow of material from the Sun known as the solar wind, which is punctuated by fast and slow streams and occasionally more energetic phenomena. There has been particular interest in how space weather affects the Earth, the Earth's weather and our satellites orbiting the Earth. One of the most energetic forms of space weather is known as Coronal Mass Ejections or CMEs, which is the sudden eruption of material from the solar surface into interplanetary space. CMEs can manifest themselves as geomagnetic storms when they interact with the Earth, which in turn can affect electrical systems and create auroras seen near the Polar Regions. Therefore, it is important to determine if and when a CME might hit the Earth or orbiting satellites.

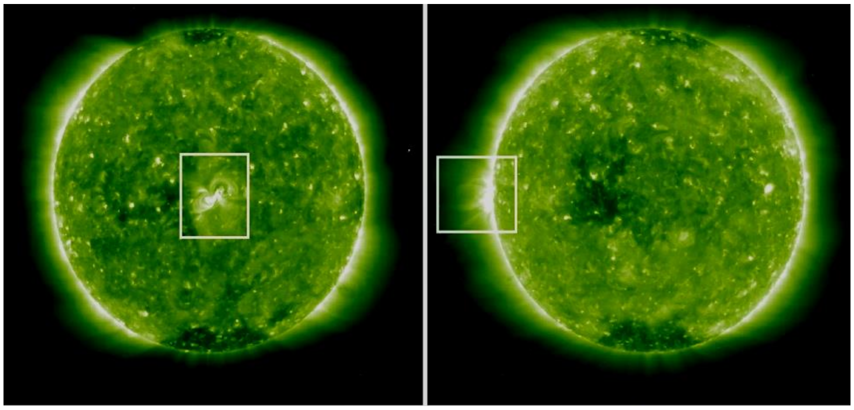

Two false colour images of the Sun, taken at the same time from the different STEREO spacecraft perspectives. The source region of a CME is highlighted by a white box; this region can be seen towards the centre of the Solar disc from one perspective and on the limb (edge) from the other. The images are taken with a EUV filter allowing images of the sun to be taken at ~1.5 Million Degrees.

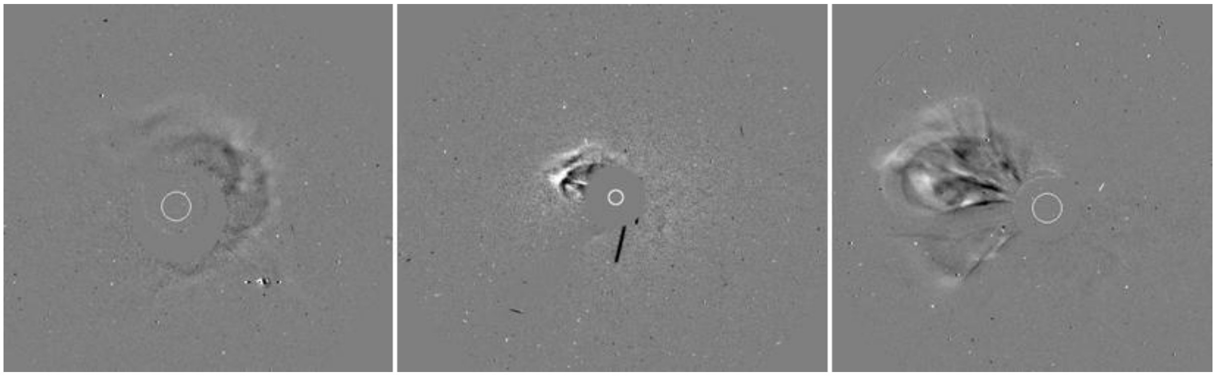

Three Images of the same Coronal Mass Ejection (CME) taken from different perspectives. Each image is taken with a coronagraph, where the bright Sun is blocked to reveal the faint surrounding interplanetary space. The images on the left and right are taken by the STEREO spacecrafts which are positioned ahead and behind the Earth in its orbit. The central image is from the Solar and Heliospheric Observatory near the Earth. The images highlight the complex structure of a CME.

In-situ observations of space weather are made from satellites, which measure ambient conditions at the position of the satellite. Such observations are made with various instruments including magnetometers, which measure the local magnetic field; and particle detectors which measure the solar wind speed, density and temperature of the ambient interplanetary conditions. CME signatures can be identified by abrupt changes in the magnetic field and particle velocities.

Researchers at ROB have linked STEREO observations to in-situ data to show that observations of CMEs made in coronagraph images close to the Sun can be used to make accurate and reliable predictions of CME transit times and directions, and more importantly if these solar storms will be Earth-directed. This work has and will be used to improve space weather forecasts produced at ROB.

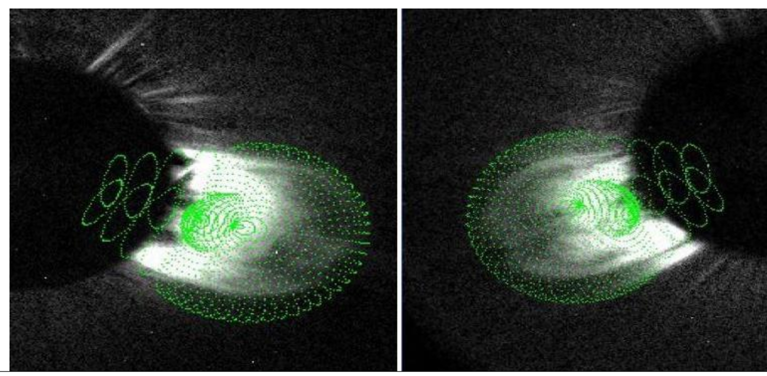

Two images of the model fitting technique used to numerically model a Coronal Mass Ejection (CME). The background black and white images show a CME viewed in coronagraph images from the STEREO satellites. The green lines outline the model fitted to the observations.

In order too predict the propagation of an individual CME, a model is fitted to observations of the eruption close to the Sun. The model provides us with information pertaining to the CME such as the direction of propagation and the CME's 3D geometrical configuration. This information can then be used to calculate the angular width, direction and speed of the CME, from which can be determined if the CME will be Earth-directed. In-situ observations made from satellites orbiting the Earth and by both STEREO spacecraft are then used to verify if the predicted arrival time and direction of a CME were correct.

The model was applied to estimate the propagation of 26 CMEs, and predicted 88% of the CMEs successfully, while a further 9% were found to lie within predicted error margins, and only one event (3%) can be considered as not successfully described by the model. Therefore, the model used to predict the arrival of CMEs can be used with a high degree of certainty when making space weather forecasts. (Further information can be obtained from Rodriguez et al. 2011).

A small-sunspot deficit in solar cycle 23

Since the last maximum of solar activity in 2000, a systematic discrepancy has appeared between the international sunspot index R_i produced at the ROB by the World Data Center "Sunspot" and several other solar indices and fluxes (see right top figure). This anomaly could be due to a flaw in the R_i index but it also corresponds to other unusual properties of the past solar cycle: internal rotation, surface flow speeds and longest minimum of activity since one century (see right bottom figure).

In order to diagnose the source of this discrepancy, we exploited the much more detailed information contained in several sunspot catalogs. For this purpose, in the context of the SoTerIA project (ended in November 2012), we worked with the two richest catalogs currently available: the Debrecen Photographic Data (DPD) and the NSO/USAF catalog available from NOAA. As those catalogs contain different but complementary information, we merged them into what must be the richest sunspot catalog currently available. In order to guarantee the completeness and accuracy of the output, this merging involved the identification of defects, inconsistencies and mismatches in either catalogs. As a complement, this validation process made partly use of the Uccle sunspot catalog based the 70-year-long ROB collection of sunspot drawings (Fig. 40), which is still in construction (completion foreseen in 2012)

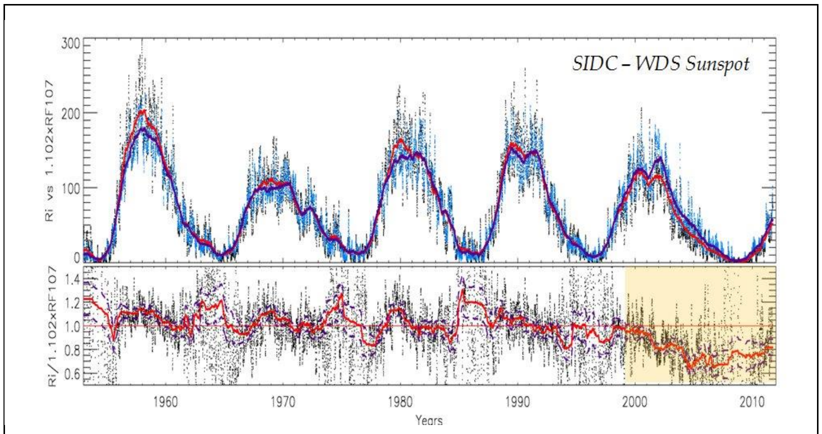

Comparison (top) and ratio (bottom) of the sunspot index R_i and the $F_{10.7cm}$ radio flux, showing the deviation after about year 2000.

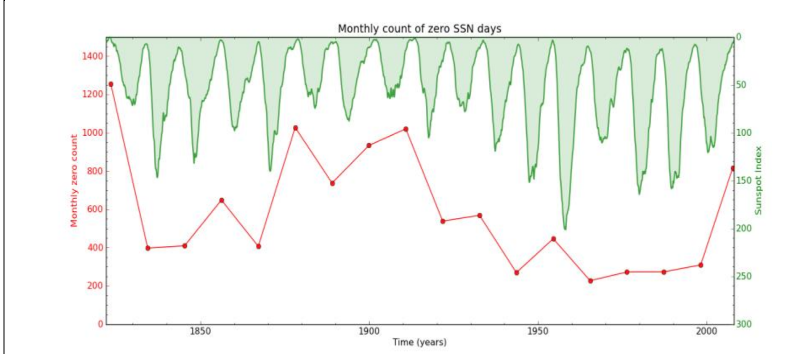

Total number of spotless days during the last 25 minima of the solar cycle. It shows the strong anti-correlation with the cycle amplitude (green, reversed scale). The last minimum exceeds all minima since the early 20th century.

Our investigations first showed that there was no intrinsic flaw in the sunspot index itself, which hinted at a true physical change in the Sun. We thus conducted extensive statistics of the populations of sunspots according to their sizes and lifetimes, considering both entire sunspot groups and also the individual sunspots forming each group. Our results show that, while the count of large groups was not different in cycle 23 compared to earlier cycles, small groups showed a strong deficit by a factor of 2 to 3 in cycle 23 (see opposite page bottom figure). This deficit also appears in the groups themselves where the relative number of small spots with the shortest lifetimes (< 2 days) has dropped in all active regions, even the large ones, in cycle 23. This transition takes place around 2000, i.e. at the time when the relation between the sunspot index R_i and other solar indices start to deviate.

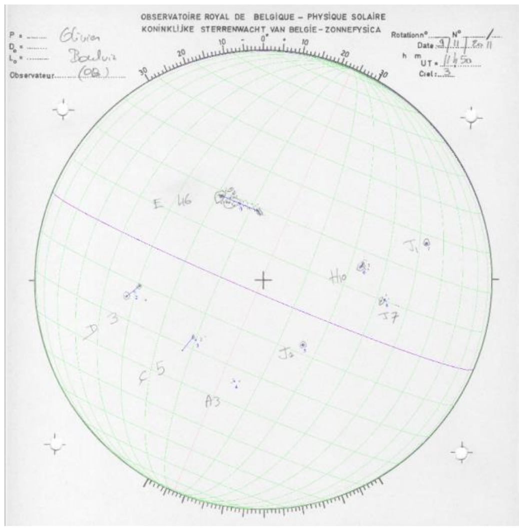

Sunspot drawing for November 9, 2011 (USET, ROB) showing the Sun at its most recent peak of activity. Screenshot with overlays from the DigiSun on-screen measuring software developed at the ROB.

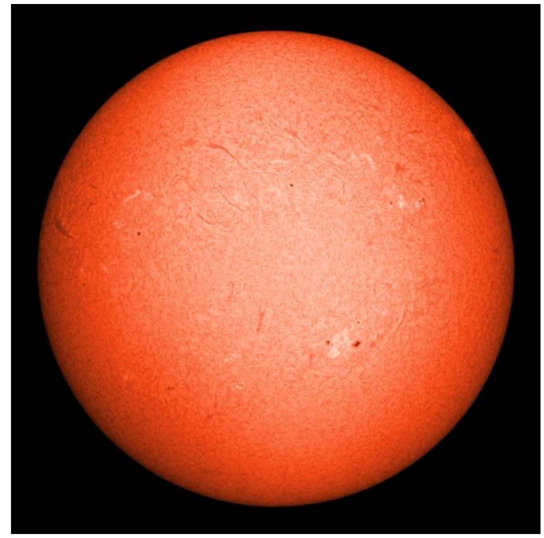

Synoptic image of the chromosphere at a fairly high level of activity on Dec.6, 2011 (Hα, USET, ROB)

Based on this detailed and independent evidence, the index deviation can then be naturally interpreted by the higher contribution of small spots in the sunspot index value compared to most other solar indices, which are heavily weighted in favor of the largest spots and magnetic fields. This strongly scale-dependent change in the distribution of sunspot magnetic fields calls for an interpretation. It matches rather well another independent observation: the steady decline of the average magnetic field strength in the core of sunspots reported by Penn & Livingston (2009, 2011). Both effects are not reproduced by the current flux transport dynamo models of the solar cycle. They may involve a distributed dynamo effect, not only confined deep inside the Sun, but with an additional component closer to the surface and acting on small-scale magnetic fields.

Further investigations of such long-term changes in the regime of solar activity will rely entirely on past and present synoptic observations, such as the white-light and Hα photographic and CCD images routinely produced at the ROB, by the Uccle Solar Equatorial Table (USET) (see top right figure).

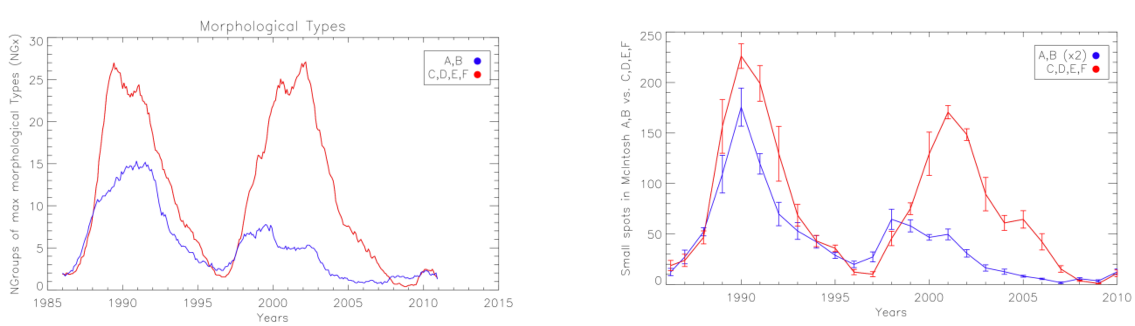

Count of small sunspot groups (A,B, in blue) and large sunspot groups (C,D,E,F, in red) during cycles 22 and 23 (left plot). Count of small spots inside groups on the same period (right plot). Both show a strong deficit affecting only the small spots.

Detection and Tracking of Active Regions and Coronal Holes

Accurate determination of Active Regions and Coronal Holes properties on coronal images is important for a wide range of applications. Active regions appear as bright regions on X-rays and EUV images. As regions of locally increased magnetic flux, they are the main source of solar eruptions. A catalog describing their key parameters such as location, shape, area, mean, and integrated intensity allows for example to relate those parameters to the occurrence of solar eruptions. Coronal holes on the other hand appear as relatively dark regions in X-rays and EUV images and therefore are typically defined as regions of low emission in the solar corona. There is a strong association between coronal holes and high-speed solar wind streams which has been known since the 1970s. Coronal holes are usually identified as the sources of the fast wind from where the wind flows out in the corona and is accelerated in open expanding magnetic funnels. Solar eruptions and fast solar wind can cause several problems for technologies on Earth and in space, and can endanger astronauts. In this way, the Sun causes what we call "space weather". Almost all space weather originates either from an Active Region or a Coronal Hole.

SPOCA module for Active Regions and Coronal Holes is running live at SDO-HEK!

Artist's concept image of the SDO satellite orbiting Earth. Credit: NASA

In the 1960s, NASA launched the Pioneer 6, 7, 8, and 9 spacecraft that were tasked with observing the solar wind and interplanetary magnetic fields, forming the first space-based space-weather network and recording 512 bits per second. By comparison, the recently launched *Solar Dynamics Observatory* (SDO) is relaying solar data back to Earth at a rate of 150 000 000 bits per second. With SDO returning the equivalent of an image with 4096 by 4096 pixels every second, human analysis of every image would require a large team of people working 24 hours a day.

Technological advances such as improving communication bandwidths and onboard processing power allows us to record data with a much greater cadence and spatial resolution than ever before.

However, the storage, transfer, and analysis of such a large flow of data is problematic. SDO generates around 1 TB of data per day, which is unprecedented in solar physics. Getting this volume of data to researchers around the world, as well as storing it in convenient places for analysis, is essential to make good use of it. An effective solution to the problem is to use automated feature-detection methods, which allow users to selectively acquire interesting portions of the full data set. In 2008, NASA selected a large international consortium, the Feature Finding Team to produce a comprehensive automated feature-recognition system for SDO. One of the goals of the consortium is to analyze images from SDO and to produce software modules that can keep up with the SDO data stream and detect, trace, and analyze numerous solar phenomena. The Royal Observatory of Belgium was part of the FFT consortium and was responsible for SPOCA, the module for Active Region and Coronal Hole detection.

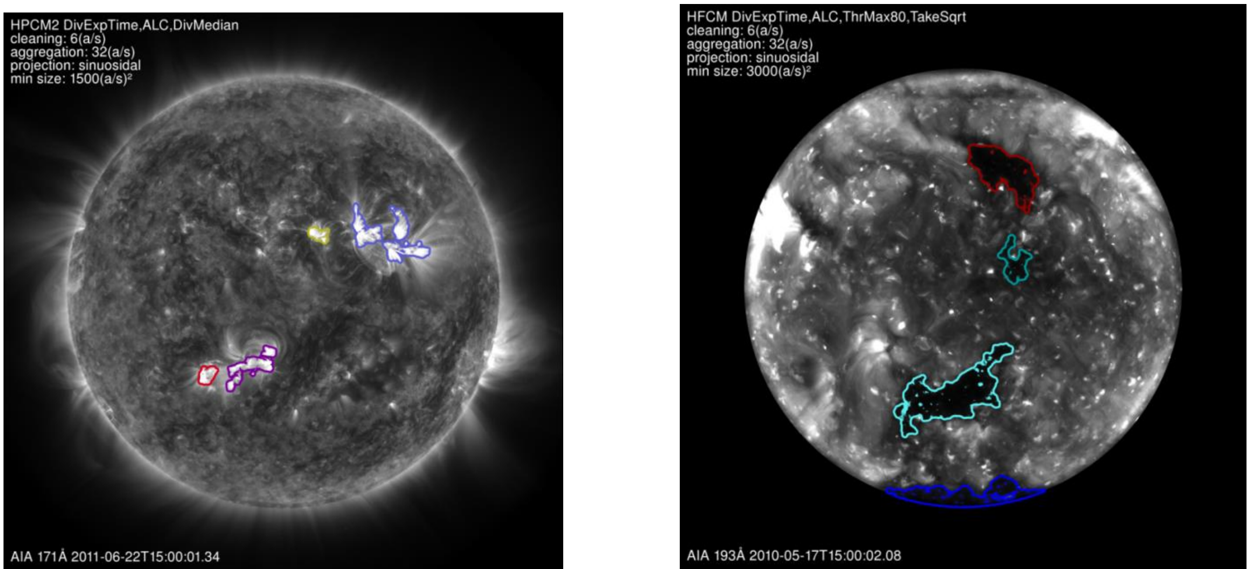

Left: overlay of Active Regions as detected by the SPOCA module on an AIA 171Å image from 22 June 2011. Right: extraction of Coronal Holes on an AIA 193Å image from 17 May 2010

In January 2011, the Active Region module of SPOCA was ready to run in near real time on SDO images at LMSAL (Lockhead Martin Solar and Astrophysical Laboratories). One year later, the Coronal Hole detection module was also made operational. Both modules now produce entries to the Heliophysics Event Knowledgebase (HEK), a database of solar features and events maintained by LMSAL. This database can be accessed through the widespread *solarsoft* library and hence permits users to locate data about individual events as well as carry out statistical studies on large numbers of events.

Since the data are analyzed in near real time as soon as they arrive at the SDO Joint Science Operations Center and have undergone basic processing, the system is able to produce timely space weather alerts and to guide the selection and production of quicklook images and movies. For example, the ESA JHelioviewer visualization tool includes the products coming from the HEK database.

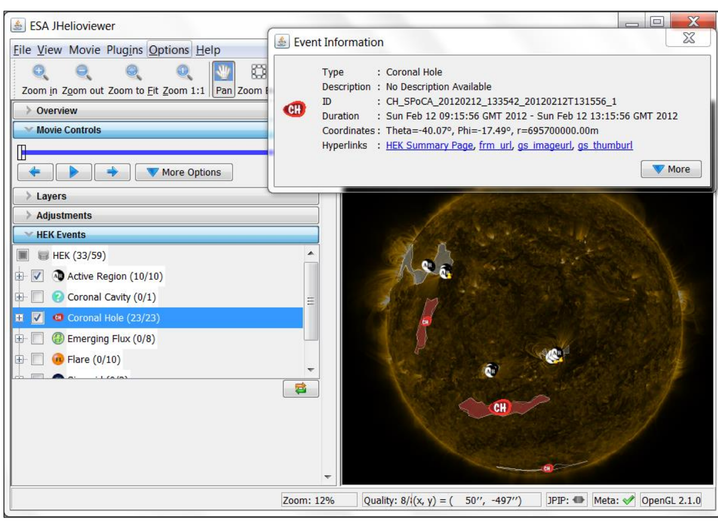

Screenshot from the ESA JHelioviewer tool. The picture on the right displays the AIA 171Å image taken on 12 February 2012 at 9:02:12 together with Active Region and Coronal Hole location and chain-code information that are recorded in the HEK. An 'Event Information' window pops up when clicking on an event or feature (here the large Coronal Hole located in the South hemisphere)

Radio Observations in Humain

The Humain station near Marche-en Famenne is a radio astronomy facility that is run by ROB since the mid-1950s. Since 2008, some of the radio telescopes on site are refurbished to host a new set of receivers dedicated to space weather monitoring and science studies linked to solar eruptive events (flares and CMEs).

A Callisto spectrograph observes the Sun since June 2008 and is following the rise of the solar activity cycle by recording an increasing number of solar radio bursts. If most of them are type III bursts linked to small reconnection events, Callisto has witnessed a series of remarkable events in the course of 2011, especially during the summer and the fall of that year.

A remarkable event: a "stationary" shock

Apart from type III already mentioned, solar radio astronomers are very keen of type II bursts, which are signatures of coronal shock waves triggered by solar flares and coronal mass ejections. The drift in frequency is an indication of the velocity of the driver of the shock, which might not be easily determined by other means.

On August 9, 2011, an X7 class flare occurred around 08:00 UT in NOAA AR 101263, close to the West solar limb. The flare was accompanied by a fast halo CME and a type II burst indicating that a coronal shock wave propagated in the wake of the CME or of a blast wave produced by the flare. We clearly see the type II burst around 08:03 UT (see figure on opposite page).

However, a minute and half later, higher up in the corona, an unusual shock signature can be observed (top right panel of the opposite figure) We suppose it's a shock signature since we do see fine structures often detected in classical type IIs, which are called "herringbones". They are "type III-like" signatures of electron beams accelerated at the shock both in sunward and anti-sunward directions, which results in opposite drifting individual bursts. These are clearly seen in this event (two red lines are drawn to guide the eyes).

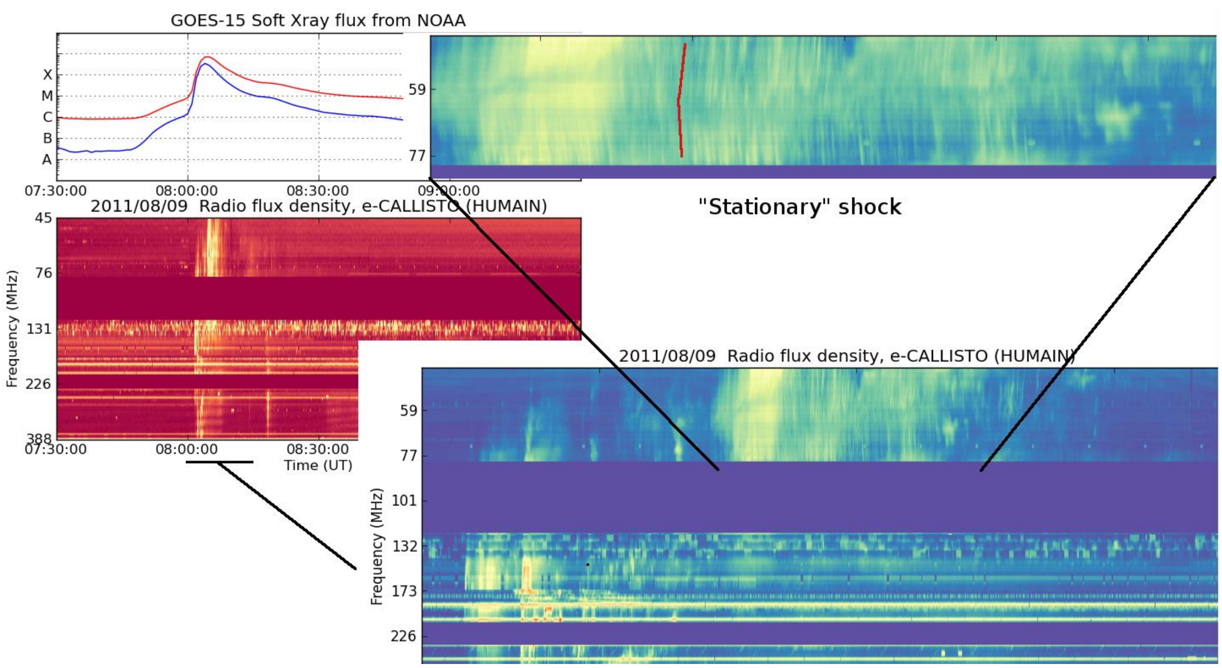

Flare event of Aug. 9, 2011. On the top right figure, sunward and anti-sunward directions are shown in red to guide the eye

Very few events of this kind have been observed so far, and the exact nature of the associated shock is still not understood, especially so high in the corona. At higher frequencies, the concept of a "termination shock" occurring in a specific reconnection geometry has been invoked, but it's not clear yet if this can be transposed to the frequency range of this event.

Data from the Callisto instrument in Humain are available on the website http://sidc.be/humain within 15 minutes. Quicklook files, combined with GOES light curves are automatically produced.

Other highlights and prospects

A new spectrograph, called Phoenix 2, will be put in operation in 2012 in Humain, expanding the frequency coverage towards the microwave range (lower down in the solar atmosphere). The telescope that will be "plugged" to this receiver had to be adapted to host a new focal plane unit. In parallel, an automatic control system prototype has been designed to track the Sun every day, without human interaction. This is needed for microwave observations, as the beam size of the telescope is decreasing with frequency.

Long-term observations will be possible if the site remains as free of interferences as possible. In 2011, a wind turbine project, within walking distance of the station has been presented to the local authorities and to the public. Needless to say, this is a worrisome prospect, and the STCE people involved in radio observations at the station (from ROB and BISA) are carefully following this issue.

Flare event of Aug. 9, 2011. On the top right figure, sunward and anti-sunward directions are shown in red to guide the eye

The Planetarium

An exceptional Influx

In 2011 46.680 people visited the Planetarium, a record for the past few years: a 62% increase was recorded (+ 18.006 visitors) compared to 2010 and an increase of +132% (+26.554 visitors) compared to the year 2000 which marks the beginning of the new admission accounting process.

This progression is due to a large increase of the non-scholar public which can be explained by several factors: First, the installation in 2009 of a new numerical projection system for the dome which enables the Brussels Planetarium to present stunning 360° shows on the whole dome to its public. Then in 2010 the Planetarium acquired a multilingual audio system and is now able to welcome French, Dutch and English speaking visitors altogether. The opening hours were also increased and the public is now welcomed during the week, weekend and bank holidays from 10am to 6pm which represents 361 opening days per year. What's more, different shows are proposed nearly each hour during weekends and holidays and the show "Violent Universe" has become one of the public's favorite movie since its launching in December 2010. Finally a combined ticket for groups and individuals was created to visit the Atomium and Mini-Europe along with the Planetarium.

The public's global satisfaction towards the different improvements also contributed to the influx increase by word of mouth advertising.

Increase of the number of visitors

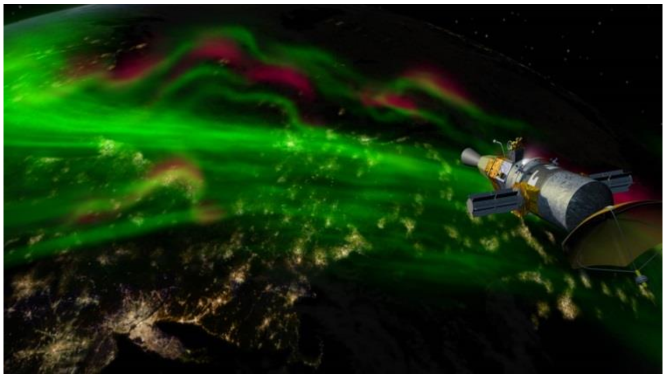

Image extracted from « Violent Universe »

"Ice Worlds", the Planetarium's new movie

In collaboration with the Belgian Institute for Space Aeronomy (BIRA-IASB), a new show was added to the Planetarium portfolio at the end of 2011. "Ice Worlds" covers several themes linked to the presence of solid water in our solar system such as moons and small icy planets, but also covers earth's poles exploration and the global warming issue.

For the 50th anniversary of Yuri Gagarine's flight, the movie "Dawn of the space age" was exceptionally projected during the spring holidays.

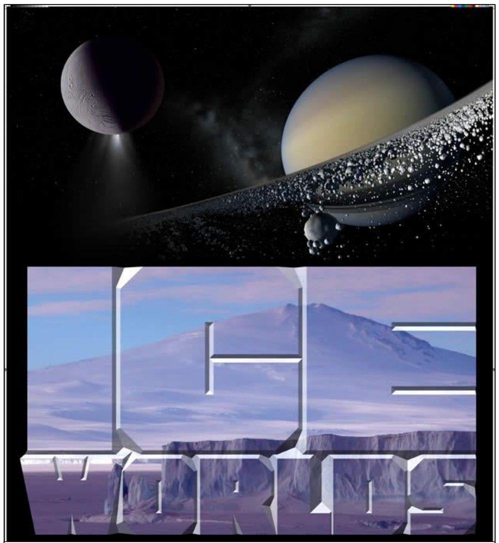

Poster of the show "Ice Worlds"

An ESERO educative workshop

ESERO Project: an efficient support for schools

In addition to the astronomy lessons given daily in primary and secondary schools by teachers, the Planetarium works actively to the valorization of science in the educational environment through the ESERO program. The European Space Agency (ESA) signed a contract with the Royal Observatory of Belgium in 2006 for the establishment of the Belgian branch of the "European Space Education Resource Office" (ESERO) in the premises of the Planetarium. The goal of this project is to favour the promotion of science subjects via strong contacts in the educational environment. The missions of the ESERO office consist of the follow-up of class projects, publication of scientific brochures, the organization of formation for teachers and future teachers, the organization of educative events on spatial subjects and the establishment of partnerships between educative authorities and the ESA

The ESERO project has reached maturity in 2011 since more than 400 teachers, 60 heads of school, 30 inspectors and 700 pupil-teachers have been trained by the Planetarium and its partners during ten training sessions which have taken place in different places across the country.

The researchers' night: between art and science

The researchers' night took place on the 23 September, and as every year, the Planetarium took part by organizing a special event on its premises and the theme "art and science" was presented through several aspects: projection of a musical film on fractals, projection of astronomical simulations on the hemispheric screen of 840 m², presentation of the night sky, broadcast of a special show at the Planetarium. Nearly 700 visitors were welcomed in a few hours during this evening.

Left: Public welcomed during the researcher's night; Right: Extract of the movie "Enigma"

Other events in 2011

- "Yuri's Night" on 21 April with Frank De Winne;
- Gezinsdag Knack on May 22;
- presentation of the book *Minnezang* by the poet Kurt de Boodts on May 28;
- European Lighting Award ceremony on October 14,
- organization of the "Darkness Night" (Nui de l'Obscurité) at Rouge-Cloître on October 15;
- Night of the museums on November 3 and on December 1.

From left to right, top: Presentation of the book Minnezang; European Lighting Award; Yuri's Night Event; bottom: Gezinsdag Knack; Darkness night at the Rouge-Cloître; Planetarium hall

Information services

Information and outreach

In 2011 the scientific information service of the ROB answered more than 750 questions from the public sent to the ROB by email, telephone or by letter or fax. As usual most were about sunset and sunrise, about astronomical phenomena (including all kind of sky objects) or calendar and time related matters. A new version of the programme to generate the standard forms of sun rise and sun set was created to output the information as a general PDF file.

Information to the media (TV, radio and written press) was given on numerous occasions, but the 'supermoon' of March, the Soyuz rocket re-entry in November, close encounters of asteroids and meteors throughout the whole year were amongst the highlights of the service.

Commenting on the Perseids in August

There was also some extra attention for the relation between Hergé and the Observatory, because of the release of the Tintin movie. A few journalists and photographers visited our site in this context. The Moulinsart Foundation visited the Observatory to gather extra information on astronomy (mostly spectroscopy) and the observatory to illustrate a special edition of "The Shooting Star".

Arend and Roland show their comet on the discovery plate

The service, sometimes with the help of other people from ROB, assisted in exhibitions and activities outside the Observatory: e.g the exhibition on Sylvain Arend in the "Musée Gaumais" in Virton (May-June 2011) or the European Institutions Open Day in Brussels on 07/05/2011.

An exhibition on Paul-Henri Stroobant (1868-1936), director of the Observatory from 1925 to 1936, was held in the Town Hall of Elsene from 31/08 to 14/09/2011. Photographs and documents on Stroobant and his epoch were shown. An academic session with lectures was organised on 07/09/2011.

Paul Stroobant, director of the Observatory from 1925 to 1936

Annex 1:
Refereed Publications
2011

1. Antoci V., Handler G., Campante T.L., Thygesen A.O., Kjeldsen H., Bedding T.R., Moya A., Kallinger T., Lüftinger T., Christensen-Dalsgaard J., Stello D., Catanzaro G., Frasca A., De Cat P., Uytterhoeven K., Bruntt H., Grigahcène A., Houdek G., Kurtz D.W., Lenz P., Kaiser A.
First evidence for solar-like oscillations in a delta Scuti star from the Kepler satellite mission
Nature 477, 570

2. Arridge C.S., and colleagues including Karatekin Ö. *Uranus Pathfinder: Exploring the Origins and Evolution of Ice Giant Planets.*
Experimental Astronomy, 113, DOI: 10.1007/ s10686-011-9251-4.

3. Baland R.-M., Van Hoolst T., Yseboodt M., and Karatekin Ö.
Titan's obliquity as evidence for a subsurface ocean.
Astronomy and Astrophysics, 530, A141, DOI: 10.1051/0004-6361/201116578.

4. Balona L.A., Pigulski A., De Cat P., Handler G., Gutiérrez-Soto J., Engelbrecht C.A., Frescura F., Briquet M., Cuypers J., Daszyńska-Daszkiewicz J., Degroote P., Dukes R.J., R. A. R.A., Green E.M., Heber U., Kawaler S., Lehmann H., Molenda-Żakowicz J., Noels A., Nuspl J., Østensen R., Pricopi D., Roxburgh I., Salmon S., Smith M.A., Suárez J.C., Suran M., Szabó R., Uytterhoeven K., Borucki W.J., Christensen-Dalsgaard J., Kjeldsen H., Koch D.G.
Kepler observations of variability in B-type stars,
MNRAS, 413, 2403-2420

5. Balona L.A., Ripepi V., Catanzaro G., Kurtz D.W., Smalley B., De Cat P., Eyer L., Grigahcène A., Leccia S., Southworth J., Uytterhoeven K., Van Winckel H., Christensen-Dalsgaard J., Kjeldsen H., Caldwell D.A., Van Cleve J., Forrest G.R.
Kepler observations of Am stars
MNRAS, 414, 792-800

6. Baire Q., Bruyninx C., Defraigne P., Legrand J.
Precise Point Positioning with ATOMIUM using IGS Orbit and Clock Products: First Results.
Bulletin of Geodesy and Geomatics, 69, 2-3, pp. 391-399.

7. M.R. Bareford, P.K. Browning, R.A.M. Van der Linden
The Flare-energy Distributions Generated by Kink-unstable Ensembles of Zero-net-current Coronal Loops
Solar Physics, 273, pp.93 – 115

8. A. Bemporad, M. Mierla, D. Tripathi
Rotation of an erupting filament observed by the STEREO EUVI and COR1 instruments
Astronomy and Astrophysics, 531, pp.

9. Bergeot N., Bruyninx C., Defraigne P., Pireaux S., Legrand J., Pottiaux E., and Baire Q.
Impact of the Halloween 2003 ionospheric storm on kinematic GPSpositioning in Europe.
GPS Solutions, 15, 2, pp. 171-180, DOI: 10.1007/s10291-010-0181-9.

10. Blomme, R.
Hot stars in the Gaia-ESO Survey
J. Phys. Conf. Ser. 328, 012019

11. Blomme, R.
Radio Observations of massive stars
Proceedings of 39th Liège Int. Astrophys. Coll. "The multi-wavelength view of hot, massive stars", Eds. P. Williams et al., Liège Royal Scientific Society 80, 67

12. Blomme, R., Mahy, L., Catala, C., Cuypers, J., Gosset, E., Godart, M., Montalban, J., Ventura, P., Rauw, G., Morel, T., and 8 coauthors
Variability in the CoRoT photometry of three hot O-type stars. HD 46223, HD 46150, and HD 46966
A&A, 533, A4

13. Bonifacio, P., Mignot, S., Dournaux, J.-L., François, P., Caffau, E., Royer, F., Babusiaux, C., Arenou, F., Balkowski, C., Bienaymé, O., Briot, D., Carlberg, R., Cohen, M., Dalton, G. B., Famaey, B., Fasola, G., Frémat, Y., Gomez, A., Guinouard, I., Haywood, M., Hill, V., Huet, J.-M., Katz, D., Horville, D., Kudritzky, R., Lallement, R., Laporte, P., de Laverny, P., Lemasle, B., Lewis, I. J., Martayan, C., Monier, R., Mourard, D., Nardetto, N., Recio Blanco, A., Robichon, N., Robin, A. C., Rodrigues, M., Soubiran, C., Turon, C., Venn, K., Viala, Y.
GYES, A
Multifibre Spectrograph for the CFHT
EAS, 45, 219-222

14. K. Bonte, C. Jacobs, E. Robbrecht, A. De Groof, D. Berghmans, S. Poedts
Validation of CME detection software (CACTus) by means of simulated data & analysis of projection effects on CME velocity measurements
Sol. Phys., 270 (1), pp.253

15. Bruyninx C., Aerts W., and Legrand J.
GPS, Data Acquisition and Analysis.
Encyclopedia of Solid Earth Geophysics, Earth Science Series, Springer, pp. 420-431, DOI: 10.1007/978-90-481-8702-7.

16. P. Chainais, V. Delouille, J.-F. Hochedez
Scale invariant images in astronomy through the lens of multifractal modeling
Proceedings, IEEE International Conference on Image Processing, , pp.1309 –1312

17. Charnoz, S., Crida A., Castillo-Rogez J., Lainey V., Dones L., Karatekin Ö., Tobie G., Mathis S., Le Poncin- Lafitte C., and Salmon J.
Accretion of Saturn mid-sized moons during the viscous spreading of young massive rings: Solving the paradox of silicate-poor rings versus silicate-rich moons.
Icarus, 216, 2, pp. 535-550, DOI: 10.1016 j.icarus.2011.09.017.

18. M.-R.L. Cioni, G. Clementini, L. Girardi, R. Guandalini, M. Gullieuszik, B. Miszalski, M.-I. Moretti, V. Ripepi, S. Rubele, G. Bagheri, K. Bekki, N. Cross, W.J.G. de Blok, R. de Grijs, J.P. Emerson , C.J.Evans, B. Gibson, E. Gonzales-Solares, M.A.T. Groenewegen, M. Irwin, V.D. Ivanov, J. Lewis, M.Marconi, J.-B. Marquette, C. Mastropietro, B. Moore, R. Napiwotzki, T. Naylor, J.M. Oliveira, M. Read , E. Sutorius , J.Th. van Loon , M.I. Wilkinson, P.R. Wood
The VMC Survey – I. Strategy and first data
A&A, 527, A116

19. F. Clette
Past and future sunspot indices: New goals for SoTerIA
Journal of Atmospheric and Solar-Terrestrial Physics, 73, Issue 2-3, pp.182-186

20. Cottenier S., Probert M., Van Hoolst T., Vanspeybroeck V., and Waroquier M.
Crystal structure prediction for iron as inner core material in heavy terrestrial planets.
Earth and Planetary Science Letters, 312, pp. 237-242, DOI: 10.1016/j.epsl.2011.09.045.

21. De Cat P.
130 positions of minor planets observed in 2011
Minor Planet Circulars Supplement 373753, 373836, 373892, 373906, 374125, 374129, 374186, 374187, 374249, 374298, 374354, 374358, 374570, 374611, 374677, 374690, 374702, 374710, 373359, 373386, 373364, 373365, 373446, 373453, 373477, 373479, 373580 (2011)

22. De Cat P.
5 positions of minor planets observed before 2011
Minor Planet Circulars Supplement 371447 (2011)

23. Decin, L., Royer, P., Cox, N.L.J., Vandenbussche, B., Ottensammer,R., Blommaert J.A.D.L., Groenewegen M.A.T., Barlow M.J., Lim T., Kerschbaum F., Posch T., Waelkens C.
Discovery of multiple dust shells beyond 1 arcmin in the circumstellar envelope of IRC +10 216 with Herschel/PACS
A&A 534, A1

24. Dehant V., Le Maistre S., Rivoldini A., Yseboodt M., Rosenblatt P., Van Hoolst T., Mitrovic M., Karatekin Ö., Marty J.C., and Chicarro A.
Revealing Mars' deep interior: Future geodesy missions using radio links between landers, orbiters, and the Earth.
Planet. Space Sci., Special Issue on 'Comparative Planetology: Venus-Earth-Mars', 59, 10, pp. 1069-1081, DOI: 10.1016/j.pss.2010.03.014.

25. Derekas A., Kiss L.L., Borkovits T., Huber D., Lehmann H., Southworth J., Bedding T.R., Balam D., Hartmann M., Hrudkova M., Ireland M.J., Kovács J., Mezö Gy., Moór A., Niemczura E., Sarty G., Szabó Gy.M., Szabó R., Telting J.H., Tkachenko A., Uytterhoeven K., Benkö J., Bryson S.T., Maestro V., Simon A.E., Stello D., Schaefer G., Aerts C., ten Brummelaar T.A., De Cat P., McAlister H.A., Maceroni C., Mérand A., Still M., Sturmann J., Sturmann L., Turner N., Tuthill P.G., Christensen-Dalsgaard J., Gilliland R.L., Kjeldsen H., Quintana E.V., Tenenbaum P., Twicken J.D.
HD181068: A Red Giant in a Triply-Eclipsing Compact Hierarchical Triple System
Science, 332, 216—218

26. L. Dolla, A.N. Zhukov
On the nature of the spectral line broadening in solar coronal dimmings
ApJ, 730, pp.113

27. Dubath P., Rimoldini L., Süveges M., Blomme J., López M., Sarro L.M., De Ridder J., Cuypers J., Guy L., Lecoeur I., Nienartowicz K., Jan A., Beck M., Mowlavi N., De Cat P., Lebzelter T., Eyer L.,
Random forest automated supervised classification of Hipparcos periodic variables,
MNRAS, 414, 2602-2617

28. Fahed, R., Moffat, A. F. J., Zorec, J., Eversberg, T., Chené, A. N., Alves, F., Arnold, W., Bergmann, T., Corcoran, M. F., Correia Viegas, N. G., Dougherty, S. M., Fernando, A., Frémat, Y., Gouveia Carreira, L. F., Hunger, T., Knapen, J. H., Leadbeater, R., Marques Dias, F., Martayan, C., Morel, T., Pittard, J. M., Pollock, A. M. T., Rauw, G., Reinecke, N., Ribeiro, J., Romeo, N., Sanchez-Gallego, J. R., Dos Santos, E. M., Schanne, L., Stahl, O., Stober, B., Stober, B., Vollmann, K., Williams, P. M.
Spectroscopy of the archetype colliding-wind binary WR 140 during the 2009 January periastron passage
MNRAS, 418, 2-13

29. U. Feldman, I.E. Dammasch, G.A. Doschek
Redshifts, widths, and radiances of spectral lines emitted by the solar transition region
Astrophysical Journal, 743, pp.165—188

30. Gowen R., and colleagues, including Dehant V. and Karatekin Ö.
Penetrators for in situ sub-surface investigations of Europa.
Adv. Space Res., 48, 4, 725-742, DOI: 10.1016/j.asr.2010.06.026.

31. M.A.T. Groenewegen, C. Waelkens, M.J. Barlow, F. Kerschbaum, P. Garcia-Lario, J. Cernicharo, J.A.D.L. Blommaert, J. Bouwman, M. Cohen, N. Cox, L. Decin, K. Exter, W.K. Gear, H.L. Gomez, P.C. Hargrave, Th. Henning, D. Hutsemekers, R.J. Ivison, A. Jorissen, O. Krause, D. Ladjal, S.J. Leeks, T.L. Lim, M. Matsuura, Y. Naze, G. Olofsson, R. Ottensamer, E. Polehampton, T. Posch, G. Rauw, P. Royer, B. Sibthorpe, B.M. Swinyard, T. Ueta, C. Vamvatira-Nakou, B. Vandenbussche, G.C. Van de Steene, S. Van Eck, P.A.M. van Hoof, H. Van Winckel, E. Verdugo, R. Wesson,
MESS (Mass-loss of Evolved StarS), a Herschel Key Program
A&A, 526, A162

32. S. Gunár, S. Parenti, U. Anzer, P. Heinzel, J. C. Vial
Synthetic differential emission measure curves of prominence fine structures: II. The SOHO/SUMER prominence of 8 June 2004
A&A, 535, pp.id.A122

33. Huang C.L., Dehant V., Liao X.H., Van Hoolst T., and Rochester M.G.
On the coupling between magnetic field and nutation in a numerical integration approach.
J. Geophys. Res., 116, B03403, DOI: 10.1029/ 2010JB007713.

34. Z. Jiang, Olivier Francis, L. Vitushkin, V. Palinkas, A. Germak, M. Becker, G. D'Agostino, Martine Amalvict, R. Bayer, M. Bilker, S. Desogus, J. Faller, R. Falk, Jacques Hinderer, C.G.L. Gagnon, Thomas Jacob, E Kalish, J. Kostelecky, C Lee, J. Liard, Y. Lokshyn, B. Luck, J. Mäkinen, S. Mizushima, N. Le Moigne, C. Origlia, E.R. Pujol, Philippe Richard, L Robertsson, D. Ruess, D. Schmerge, Y. Stus, S. Svitlov, S. Thies, C. Ullrich, Michel Van Camp, A. Vitushkin, W. Ji, Herbert Wilmes
Final report on the Seventh International Comparison of Absolute Gravimeters (ICAG 2005)
Metrologia 48, 246-260 (2011).

35. Hubrig S., Ilyin I., Schöller M., Briquet M., Morel T., De Cat P.
First magnetic field models for recently discovered magnetic beta Cephei and slowly pulsating B stars
ApJ Letters 726, L5

36. M.E. Innocenti, Giovanni Lapenta, B. Vrsnak, F. Crespon, C. Skandrani, M. Temmer, A. M. Veronig, Lapo Bettarini, S. Markidis, M. Skender
Improved forecasts of solar wind parameters using the Kalman filter
Space Weather, 9, pp.S10005

37. Jo Gottsmann, S. De Angelis, Nicolas Fournier, Michel Van Camp, S Sacks, A Linde, M. Ripepe
On the geophysical fingerprint of Vulcanian explosions
Earth and Planetary Sciences Letters 306, 98-104 (2011).

38. Jorissen A., Mayer A., Van Eck S., Ottensamer R., Kerschbaum F., Ueta T., Bergman P., Blommaert J.A.D.L., Decin L., Groenewegen M.A.T., Hron J., Nowotny W., Olofsson H., Posch Th., Sjouwerman L.O., Vandenbussche B., and Waelkens C.
X Herculis and TX Piscum: two cases of ISM interaction with stellar winds observed with Herschel
A&A 532, A135

39. Karatekin Ö., de Viron O., Lambert S., Rosenblatt P., Dehant V., Van Hoolst T., and Le Maistre S.
Atmospheric angular momentum variations of Earth, Mars and Venus at seasonal time scales.
Planet Space Sci., Special Issue on 'Comparative Planetology: Venus-Earth-Mars', 59, 10, pp. 923-933, DOI: 10.1016/j.pss.2010.09.010.

40. Konopliv A.S. , Asmar S.W., Folkner W.M. , Karatekin Ö., Nunes D.C., Smrekar S.E., Yoder C.F., and Zuber M.T.
Mars High Resolution Gravity Fields from MRO, Mars Seasonal Gravity, and Other Dynamical Parameters.
Icarus, 211, 1, pp. 401-428, DOI: 10.1016/j.icarus.20110.10.004.

41. Koot L., and Dumberry M.
Viscosity of the Earth's inner core: constraints from nutation observations.
Earth and Planetary Science Letters, 308, pp. 343-349, DOI: 10.1016/j.epsl.2011.06.004

42. Koot L., and de Viron O.
Atmospheric contributions to nutations and implications for the estimation of deep Earth's properties from nutation observations.
Geophysical Journal International, 185, pp. 1255–1265, DOI: 10.1111/j.1365-246X.2011.05026.x.

43. Lampens, P., Strigachev, A., Kim, S.-L., Rodríguez, E., López-González, M. J., Vidal-Saínz, J., Mkrtichian, D., Van Cauteren, P., Wils, P., Southworth, J., García-Melendo, E., Gómez Forellad, J. M. (2011)
Multi-site, multi-year monitoring of the oscillating Algol-type binary CT Her
A&A 534, A111

44. Lamy P., Vernazza P., Poncy J., Martinot V., Hinglais E., Canalias E., Bell J., Cruikshank D., Groussin O., Helbert J., Marzari F., Morbidelli A., Rosenblatt P., and Sierks H.
Trojans' Odyssey: Unveiling the early history of the Solar system.
Experimental Astronomy, DOI: 10.1007/s10686-011-9253-2.

45. Giovanni Lapenta, Lapo Bettarini
Self-consistent seeding of the in- terchange instability in dipolarization fronts
Geophysical Research Letters, 38, pp.CiteID L11102

46. Giovanni Lapenta, Lapo Bettarini
Spontaneous transition to a fast 3D turbulent reconnection regime
Europhysics Letters, 93, pp.65001

47. S. Landi, Lapo Bettarini
Three-Dimensional Simulations of Magnetic Reconnection with or Without Velocity Shears
Space Science Reviews, Online First, pp.

48. Le Bars M., Wieczorek M.A., Karatekin Ö., Cébron D., and Laneuville M.
An impact-driven dynamo for the early Moon.
Nature, 479, pp. 215-218, DOI: 10.1038/ nature10565, 2011.

49. L. Lefèvre, F. Clette
A global small-sunspot deficit at the base of the index anomalies of solar cycle 23
A&A, 536, pp.L11

50. Legrand J., Bruyninx C., and Bergeot N.
Results and Comparisons of a Local and a Regional Reprocessed GNSS Network
Bulletin of Geodesy and Geomatics, 69, 2-3, pp. 257-267.

51. Lehmann H., Tkachenko A., Semaan T., Gutiérrez-Soto J., Smalley B., Briquet M., Shulyak D., Tsymbal V., De Cat P.
Spectral analysis of Kepler SPB and beta Cep candidate stars
A&A 526, A124

52. Lobel, A., De Greve, J.-P., van Rensbergen, W.,
Preface - Stellar Atmospheres in the Gaia Era,
J. Phys. Conf. Ser. 328, 011001

53. Lobel, A.,
Stellar Atmospheres in the Gaia Era (Conference Review),
J. Phys. Conf. Ser. 328, 012027

54. Lobel, A.,
Oscillator Strength Measurements from Stellar Spectra,
Can. J. Phys., 89, 395

55. Lobel, A., Toalá, J.A., Blomme, R.
3-D Radiative Transfer Modeling of Structured Winds in Massive Hot Stars with Wind3D
Proceedings of 39th Liège Int. Astrophys. Coll. "The multi-wavelength view of hot, massive stars", Eds. P. Williams et al., Liège Royal Scientific Society 80, 42

56. Mahy, L.; Gosset, E.; Baudin, F.; Rauw, G.; Godart, M.; Morel, T.; Degroote, P.; Aerts, C.; Blomme, R.; Cuypers, J.; Noels, A.; Michel, E.; Baglin, A.; Auvergne, M.; Catala, C.; Samadi, R.,
Plaskett's Star: Analysis of the CoRoT photometric data,
Astronomy & Astrophysics, 525, A101

57. Maisonneuve F., Pollard K.R., Cottrell P.L., Wright D.J., De Cat P., Mantegazza L., Kilmartin P.M., Suárez J.C., Rainer M., Poretti E.
First frequency analysis and pulsational mode identification of two gamma Doradus stras: HD40745 and HD189631
MNRAS 415, 2977

58. P. Malinowski, J.-Y. Duboz, Piet de Moor, J John, Kyriaki Minoglou, N. Srivastava, F. Semond, Eric Frayssinet, B. Giordanengo, A. BenMoussa, U. Kroth, C. Laubis, R. Mertens, C. Van Hoof
AlGaN-on-Si-based 10 μm pixel-to-pixel pitch hybrid imagers for the EUV range
Electron Device Letters, 32, pp.1561-1563

59. P. Malinowski, J.-Y. Duboz, Piet de Moor, Kyriaki Minoglou, J John, B. Giordanengo, A. BenMoussa, R. Mertens, C. Van Hoof
Extreme ultraviolet detection using AlGaN-on-Si inverted Schottky photodiodes
Applied Physics Letters, 98, pp.14104

60. S. Markidis, Giovanni Lapenta, Lapo Bettarini, M. Goldman, D. Newman, L. Andersson
Kinetic simulations of magnetic reconnection in presence of a background O+ population
Journal of Geophysical Research, 116, pp.CiteID A00K16

61. Martayan, C., Zorec, J., Baade, D., Frémat, Y., Fabregat, J., Ekström, S.
Evolution of massive Be and Oe stars at low metallicity towards the Long Gamma Ray bursts
BSRSL, 80, 285-290

62. Martayan, C., Blomme, R., …, Frémat, Y., Lobel, A., …
X-shooter, NACO, and AMBER observations of the LBV Pistol Star
Proceedings of 39th Liège Int. Astrophys. Coll. "The multi-wavelength view of hot, massive stars", Eds. P. Williams et al., Liège Royal Scientific Society 80, 400

63. Mayer A., Jorissen A., Kerschbaum F., Mohamed S., van Eck S., Ottensamer R., Blommaert J.A.D.L., Decin L., Groenewegen M.A.T., Posch Th., Vandenbussche B., Waelkens C.
Herschels view into Mira's head
A&A 531, L4

64. M. Mierla, I. Chifu, B. Inhester, L. Rodriguez, A.N. Zhukov
Low polarised emission from the core of the 31 August 2007 CME
Astron. Astrophys., 530, pp.

65. M. Mierla, B. Inhester, L. Rodriguez, S. Gissot, A.N. Zhukov, N. Srivastava
On 3D Reconstruction of Coronal Mass Ejections: II. Longitudinal Width Analysis of 31 August 2007 Event
J. Atmos. Sol.-Terr. Phys., 73, pp.1166-1172

66. Miszalski B., Napiwotzki R., Cioni M.-R.L., Groenewegen M.A.T., Oliveira J.M., Udalski A.
The VMC survey II. A multi-wavelength study of LMC planetary nebulae and their mimics
A&A 531, A157

67. Mocquet A., Rosenblatt P., Dehant V., and Verhoeven O.
The deep interior of Venus, Mars, and the Earth: a brief review and the need for planetary surface-based measurements.
Planet. Space Sci., Special Issue on 'Comparative Planetology: Venus-Earth-Mars', 59(10), pp. 1048-1061, DOI: 10.1016/j.pss.2010.02.002

68. Noyelles, B, Karatekin Ö., and Rambaux N.
The rotation of Mimas.
Astronomy and Astrophysics, 536, id. A61, DOI: 10.1051/0004-6361/201117558.

69. O'Dell C.R., Ferland G.J., Porter R.L., van Hoof P.A.M.
Physical Conditions in Barnard's Loop, Components of the Orion-Eridanus Bubble, and Implications for the WIM Component of the ISM
ApJ, 733, 9

70. J.M. Pasachoff, E.D. Tingle, I.E. Dammasch, A. Sterling
Simultaneous Observations of the Chromosphere with TRACE and SUMER
Solar Physics, 268, pp.151—163

71. J.M. Pasachoff, V. Rusin, H. Druckmullerova, M. Saniga, M. Lu, C. Malamut, D.B. Seaton, L. Golub, A. J. Engell, S. Hill, R. Lucas
Structure and Dynamics of the 2010 July 11 Eclipse White-light Corona
Astrophysical Journal, 734, pp.114 (10pp)

72. Pauwels, T.
111 positions of asteroids
MPS 368881, 369596, 371411, 371447, 373351, 373359, 373430, 373456, 373462, 373477, 374090, 374585, 375476, 375497, 382330, 384631, 385171, 385378, 387244, 387779, 388645, 398343.

73. Pham L.B.S., Karatekin Ö., and Dehant V.
Effects of impacts on the atmospheric evolution: comparison between Mars, Earth and Venus.
Planet. Space Sci., 59, 10, pp. 1087-1092, DOI: 10.1016/j.pss.2010.11.010.

74. Pfyffer G., Van Hoolst T., and Dehant V.
Librations and Obliquity of Mercury from the BepiColombo radio-science and camera experiments.
Planet. Space Sci., 59, 9, pp. 848-861, DOI: 10.1016/j.pss.2011.03.017.

75. T. Podladchikova, R.A.M. Van der Linden
Peak Sunspot Number for Solar Cycle 24
Journal of Space Weather and Space Climate, 1, pp.A01

76. Pottiaux E., Brockmann E., Bruyninx C., and Söhne W.
The EUREF-EUMETNET Collaboration: First Experience and Potential Benefits.
Bulletin of Geodesy and Geomatics, Vol. LXVIII, N°3, pp. 269-288.

77. Rajka Jurdana-Sepic, R. Brajsa, H. Woehl, A. Hanslmeier, I. Poljancic, L. Svalgaard, S. Gissot
A relationship between the solar rotation and activity in the period 1998-2006 analysed by tracing small bright coronal structures in SOHO-EIT images
Astronomy and Astrophysics, 534, pp.A17

78. Rambaux N., Van Hoolst T., and Karatekin Ö.
Librational response of Europa, Ganymede, and Callisto with an ocean for a non-keplerian orbit.
Astronomy and Astrophysics, 527, A118, DOI: 10.1051/0004-6361/201015304.

79. Rambaux N., Castillo-Rogez J., Dehant V., and Kuchynka P.
Constraining Ceres' interior from its Rotational Motion.
Astron. Astrophys., 535, A43, 10 pages, DOI: 10.1051/0004-6361/201116563.

80. Raskin, G., van Winckel, H., Hensberge, H., Jorissen, A., Lehmann, H., Waelkens, C., Avila, G., de Cuyper, J.-P., Degroote, P., Dubosson, R., Dumortier, L., Frémat, Y., Laux, U., Michaud, B., Morren, J., Perez Padilla, J., Pessemier, W., Prins, S., Smolders, K., van Eck, S., Winkler, J.
HERMES: a high-resolution fibre-fed spectrograph for the Mercator telescope
A&A, 526, 69

81. Rivoldini A., Van Hoolst T., Verhoeven O., Mocquet A., and Dehant V.
Geodesy constraints on the interior structure of Mars.
Icarus, 213, pp. 451-472, DOI: 10.1016 /j.icarus.2011.03.024.

82. Robert, V.; de Cuyper, J.-P.; Arlot, J.-E.; de Decker, G.; Guibert, J.; Lainey, V.; Pascu, D.; Winter, L.; Zacharias, N.
A new astrometric reduction of photographic plates using the DAMIAN digitizer: improving the dynamics of the Jovian system
MNRAS 415, 701-708

83. L. Rodriguez, M. Mierla, A.N. Zhukov, M. West, E. Kilpua
Linking remote-sensing and in situ observations of coronal mass ejections using STEREO
Solar Physics, 270, pp.561-573

84. Rosenblatt P.
The origin of the Martian moons revisited
Astronomy and Astrophysics Review, 19, 1, pp. 19-44.

85. D.B. Seaton, M. Mierla, D. Berghmans, A.N. Zhukov, L. Dolla
SWAP-SECCHI Observations of a Mass-loading Type Solar Eruption
ApJ Letters, 727 (Iss 1), pp.L10 (5pp)

86. Sloan G.C., Hony S., Smolders K., Decin L., Zijlstra A.A., Feast M.W., van Wyk F., van Loon J.Th., Groenewegen M.A.T., Sahai, R.
The identification of probable SiS emission at 13-14 micron in the spectra of Galactic S-stars
ApJ 729, 121

87. Sordo, R., Vallenari, A., Tantalo, R., Liu, C., Smith, K., Allard, F., Blomme, R., Bouret, J.-C., Brott, I., de Laverny, P., Edvardsson, B., Frémat, Y. and 11 coauthors
Stellar libraries for Gaia
J. Phys. Conf. Ser. 328, 012006

88. Tokano T., Van Hoolst T., and Karatekin Ö.
Polar motion of Titan forced by the atmosphere.
Journal of Geophysical Research – Planets, 116, E05002, DOI: 10.1029/2010JE003758.

89. Torres, K. B. V., Lampens, P., Frémat, Y., Hensberge, H., Lebreton, Y., Skoda, P.,
Spectra disentangling applied to the Hyades binary Theta² Tauri AB: new orbit, orbital parallax and component properties
A&A, 525, 50

90. Uttenthaler, S., van Stiphout, K., Voet, K., van Winckel, H., van Eck, S., Jorissen, A., Kerschbaum, F., Raskin, G., Prins, S., Pessemier, W., Waelkens, C., Frémat, Y., Hensberge, H., Dumortier, L., Lehmann, H.
The evolutionary state of Miras with changing pulsation periods
A&A, 531, 88

91. Uytterhoeven, K.; Moya, A.; Grigahcène, A.; Guzik, J. A.; Gutiérrez-Soto, J.; Smalley, B.; Handler, G.; Balona, L. A.; Niemczura, E.; Fox Machado, L.; Benatti, S.; Chapellier, E.; Tkachenko, A.; Szabó, R.; Suárez, J. C.; Ripepi, V.; Pascual, J.; Mathias, P.; Martín-Ruíz, S.; Lehmann, H.; Jackiewicz, J.; Hekker, S.; Gruberbauer, M.; García, R. A.; Dumusque, X.; Díaz-Fraile, D.; Bradley, P.; Antoci, V.; Roth, M.; Leroy, B.; Murphy, S. J.; De Cat, P.; Cuypers, J.; Kjeldsen, H.; Christensen-Dalsgaard, J.; Breger, M.; Pigulski, A.; Kiss, L. L.; Still, M.; Thompson, S. E.; van Cleve, J.
The Kepler characterization of the variability among A- and F-type stars. I. General overview,
A&A, 534, A125

92. Michel Van Camp, Olivier de Viron, Hans-Georg Scherneck, Klaus-G. Hinzen, Simon D.P. Williams, Thomas Lecocq, Yves Quinif, Thierry Camelbeeck
Repeated absolute gravity measurements for monitoring slow intraplate vertical deformation in Western Europe
Journal of Geophysical Research 116, B08402 (2011)

93. T. Van Doorsseleare, A. De Groof, J. Zender, D. Berghmans, M. Goossens
LYRA Observations of Two Oscillation Modes in a Single Flare
ApJ, 740 (Iss 2), pp.90

94. C. Verbeeck, P. Higgins, T. Colak, F. Watson, V. Delouille, B. Mampaey, R. Qahwaji
A multi-wavelength analysis of active regions and sunspots by comparison of automatic detection algorithms
Solar Physics, 283, pp.67-95

95. Olivier de Viron, Michel Van Camp, Olivier Francis
Revisiting Absolute Gravimeter Intercomparisons
Metrologia 48, 290-298 (2011).
Alternatieve koppeling

96. Volpi, D.
Modelling the synchrotron emission from O-star colliding wind binaries
Proceedings of 39th Liège Int. Astrophys. Coll. "The multi-wavelength view of hot, massive stars", Eds. P. Williams et al., Liège Royal Scientific Society. 80, 733-737

97. Y.M. Wang, E. Robbrecht
Asymmetric Sunspot Activity and the Southward Displacement of the Heliospheric Current Sheet
Astrophysical Journal, 736, pp.136-147

98. Y.M. Wang, E. Robbrecht, K. Muglach
The Evolution of Dark Canopies Around Active Regions
Astrophysical Journal, 733, pp.20-27

99. M. West, A.N. Zhukov, L. Dolla, L. Rodriguez
Coronal seismology using EIT waves: estimation of the coronal magnetic field strength in the quiet Sun
Apj, 730, pp.122

100. Wils, P., Panagiotopoulos, K.; Van Wassenhove, J.; Ayiomamitis, A.; Nieuwenhout, F.; Robertson, C. W.; Vanleenhove, M.; Hambsch, F.-J.; Hautecler, H.; Pickard, R. D.; Baillien, A.; Staels, B.; Kleidis, S.; Lampens, P.; Van Cauteren, P. (2011)
Photometry of High-Amplitude Delta Scuti Stars (HADS)
Information Bulletin on Variable Stars, 6015, 1

101. Wright, D.J., Chené A.-N., De Cat P., Marois C., Mathias P., Macintosh B., Isaacs J., Lehmann H., Hartmann M.
Determination of the inclination of the multi-planet hosting star HR8799 using asteroseismology
ApJ Letters, 728, L20-L24

102. Young, P. R., Feldman, U., & Lobel, A.,
Forbidden and Intercombination Lines of RR Telescopii: wavelength measurements and energy level,
ApJS, 196, 23

103. Yu.S. Shugai, I.S. Veselovsky, D.B. Seaton, D. Berghmans
Hierarchical approach to forecasting recurrent solar wind streams
Solar System Research, 45 (Iss 6), pp.546-556

104. A.N. Zhukov, *EIT Wave Observations and Modeling in the STEREO Era*
J. Atmos. Sol.-Terr. Phys., 73, pp.1096—1116

105. Zorec, J., Frémat, Y., Domiciano de Souza, A., Delaa, O., Stee, P., Mourard, D., Cidale, L., Martayan, C., Georgy, C., Ekström, S.
Differential rotation in rapidly rotating early-type stars. I. Motivations for combined spectroscopic and interferometric studies
A&A, 526, 87

Annex 2:
Human Resources
2011

Algemeen directeur/ Directeur général Van der Linden Ronald

Vastbenoemd wetenschappelijk personeel / Personnel scientifique statutaire

Name/Nom	Functie/Fonction	Name/Nom	Functie/Fonction
Alexandre Pierre	Premier assistant	Groenewegen Martin	Eerstaanwezend assistent
Alvarez Rodrigo	Premier assistant	Hochedez Jean-François	Premier assistant
Berghmans David	Werkleider	Lampens Patricia	Departementshoofd
Blomme Ronny	Eerstaanwezend assistent	Lecocq Thomas	Assistant-stagiaire
Bruyninx Carine	Eerstaanwezend assistent	Legrand Juliette	Assistant-stagiaire
Camelbeeck Thierry	Werkleider	Pauwels Thierry	Afdelingshoofd
Clette Frédéric	Premier assistant	Robbrecht Eva	Assistant-stagiaire
Collin Fabienne	Premier assistant	Roosbeek Fabian	Premier Assistant
Cuypers Jan	Eerstaanwezend assistent	Van Camp Michel	Chef de travaux
De Cat Peter	Eerstaanwezend assistent	Van De Steene Griet	Eerstaanwezend assistent
Defraigne Pascale	Premier assistant	Van Hoolst Tim	Werkleider
Dehant Véronique	Chef de Section	Vanneste Kris	Eerstaanwezend assistent
Frémat Yves	Assistant	Yseboodt Marie	Assistant

Vastbenoemd technisch en administratief personeel / Personnel technique et administratif statutaire

Name/Nom	Functie/Fonction	Name/Nom	Functie/Fonction
Asselberghs Somnina	Technisch deskundige	Van Camp Lydia	Technisch deskundige
Boulvin Olivier	Expert technique	Van Damme Daniel	Technisch deskundige
Bukasa Baudouin	Expert technique	Van De Putte William	Technisch deskundige
Castelein Stefaan	Technisch deskundige	Van Der Gucht Ignace	Technisch deskundige
Coene Yves	Expert technique	Vandekerckhove Joan	Technisch deskundige
Driegelinck Eddy	Expert technique	Vandercoilden Leslie	Expert technique
Dumortier Louis	Expert ICT	Vanraes Stéphane	ICT deskundige
Duval David	Expert ICT	Vermeiren Katinka	ICT deskundige
Ergen Aydin	Expert technique	Van de Meersche Olivier	Expert Financier
Frederick Bert	Expert technique	Wintmolders Sabrina	Administratief deskundige
Hendrickx Marc	Expert technique	Barthélémy Julie	Chef technicien de la recherche
Herreman David	Expert ICT	Bizerimana Philippe	Assistant technique
Langenaken Hilde	Technisch deskundige	Brebant Christian	Assistant administratif
Martin Henri	Expert technique	Bruyninckx Martine	Administratief assistent
Mesmaker Dominique	Expert technique	Danloy Jean-Marie	Assistant administratif
Moyaert Ann	ICT deskundige	Depasse Béatrice	Assistant administratif
Renders Francis	Technisch deskundige	De Wachter Rudi	Technisch assistent
Somerhausen André	Expert ICT	Feldberg Liesbeth	Administratief assistent
Strubbe Marc	Technisch deskundige	Consiglio Sylvia	Administratief medewerker
Jacques Jean-Claude	Assistant technique	Jans Thimoty	Attaché A1
Janssens Paul	Assistant technique	Kochuyt Anne-Lize	Attaché A1
Lemaitre Olivier	Assistant technique	Rezabek Oleg	Attaché A1
Trocmet Cécile	Assistant administratif	Rogge Vincent	Attaché A1/A2
Van Den Brande	Technisch assistent	De Knijf Marc	Attaché A2
Theophilis		Dufond Jean-Luc	Attaché A2
Vanden Elshout Ronny	Assistant technique	Milis André	Attaché A2
Verbeeren Anja	Administratief assistent		

Contractueel wetenschappelijk personeel / Personnel scientifique contractuel

Name/Nom	Functie/Fonction	Name/Nom	Functie/Fonction
Aerts Wim	Assistent	Magdalenic Jasmina	Assistant
Baire Quentin	Assistant	Marqué Christophe	Assistant
Benmoussa Ali	Premier assistant	Mitrovic Michel	Assistant
Bergeot Nicolas	Assistant	Nicula Bogdan	Assistant
Bettarini Lapo	Assistent	Parenti Suzanna	Premier assistant
Beuthe Mikael	Assistant	Pfyffer Gregor	Assistant
Bourgoignie Bram	Assistant-stagiaire	Podladchikova Olena	Premier assistant
Cabanas Carlos	Assistant	Pottiaux Eric	Assistant
Callebaut Benoît	Assistant	Pylyser Eric	Assistant
Caudron Corentin	Assistant	Rivoldini Attilio	Assistant
Champagne Georges	Assistant	Robyns Sophie	Assistent-stagiaire
Chevalier Jean-Marie	Assistant	Rodriguez Luciano	Assistant
Dammasch Ingolf	Assistant	Rosenblatt Pascal	Premier assistant
De Cuyper Jean-Pierre	Eerstaanwezend assistent	Seaton Daniel	Assistant
Delouille Véronique	Premier assistant	Stegen Koen	Assistent
D'Huys Elke	Assistent	Torres Kelly	Assisstant
Dolla Laurent	Assistant	Van Hoof Peter	Assistent
Dominique Marie	Assistant	Van Hove Bart	Assistent
Garcia Moreno David	Assistant	Vanlommel Petra	Eerstaanwezend assistent
Giordanengo Boris	Premier assistant	Van Noten Koen	Assistent
Gissot Samuel	Assistant	Verbeeck Francis	Assistent/ Eerstaanwezend assistent
Gullieuszik Marco	Assistant		
Joukov Andrei	Premier assistant	Verbeeck Koen	Assistant
Karatekin Ozgur	Assistant	Verbruggen Wim	Assistent-stagiaire
Knuts Elisabeth	Assistant	Verdini Andrea	Assistant
Kretzschmar Matthieu	Premier assistant	Verstringe Freek	Assistent
Kudryashova Maria	Assistant	Vleminckx Bart	Assistent
LeMaistre Sébastien	Assistant	Volpi Delia	Assistant
Lefevre Laure	Assistant	Wauters Laurence	Premier assistant
Lisnichenko Pavlo	Assistant-stagiair	West Matthew	Assistant
Lobel Alex	Eerstaanwezend assistent	Zhu Ping	Assistant
Lombardini Denis	Assistant		

Wetenschappelijke personeel met externe beurzen / Personnel scientifique sur bourses externes

Name/Nom	Functie/Fonction	Name/Nom	Functie/Fonction
Hees Aurélien	Boursier FRIA	Pham Le Binh San	Boursier FNRS
Kusters Dimitri	Boursier FRIA	Trinh Antony	Boursier FNRS
Baland Rose-Marie	Boursier FRIA		

Contractueel technisch en administratief personeel / personnel technique et administrative contractuel

Name/Nom	Functie/Fonction	Name/Nom	Functie/Fonction
Bastin Véronique	Expert technique	Rapagnani Giovanni	Attaché A1
Coeckelberghs Hans	Technisch deskundige	Reghif Harraz Mohammed	Collaborateur technique
Cornet Denis	Attaché A1	Sayer Amina	Collaborateur technique
De Decker Georges	Attaché A2	Semeraro Vanessa	Administratief assistant
De Dobbeleer Rudy	Technisch assistant	Smet Gert	Technisch assistent
De Vos Frédéric	Expert ICT	Sojic Marko	Attaché A1
El Amrani Malika	Collaborateur technique	Thienpont Emmanuel	ICT deskundige
Esperito Santo Marco	Collaborateur technique	Trindade Josefina	Collaborateur technique
Feldberg Liesbeth	Administratief assistent	Trocmet Cécile	Assistant administratif
Geerts Ellen	Attaché A1	Vandercoilden Myriam	Assistant administratif
Gonzales Sanchez Bénédicte	Collaborateur technique	Vandeperre Arnold	Technisch assistent
Herman Viviane	Collaborateur technique	Vander Putten Wim	Expert ICT
Hernando Ana Maria	Assistant administratif	Vandersyppe Anne	Administratief expert
Ipuz Mendez Adriana	Collaborateur technique	Van Elder Sophie	Attaché A1
Kurudere Hulya	Technisch medewerker	Van Hemelryck Eric	Attaché A2
Lagmara Nadia	Administratief medewerker	Verbeeck Koen	Assistent SW1
Mampaey Benjamin	Attaché A2	Vermeylen Jacqueline	Collaborateur technique
Motte Philippe	Collaborateur technique	Wellens Véronique	Attaché A1
Mouling Ilse	Administratief assistent	Wijns Erik	Technisch medewerker
Noel Jean-Philippe	Expert technique	Willems Sarah	Attaché A2

Gedetacheerd personeel / Personnel détaché

Naam/Nom	Functie/Fonction	Contract
Vanhassel Luc	Adjunct technicus	BIPT (tot 31/01/2012)
De Rijcke Hendrick	Leraar	Onderwijs Vlaanderen